

Skip-Vision: Efficient and Scalable Acceleration of Vision-Language Models via Adaptive Token Skipping

Weili Zeng

MoE Key Lab of Artificial Intelligence, AI Institute
Shanghai Jiao Tong University

zwl666@sjtu.edu.cn

Ziyuan Huang

Ant Group

ziyuan.huang@u.nus.edu

Kaixiang Ji

Ant Group

kaixiang.jkx@antgroup.com

Yichao Yan

MoE Key Lab of Artificial Intelligence, AI Institute
Shanghai Jiao Tong University

yanyichao@sjtu.edu.cn

Abstract

Transformer-based models have driven significant advancements in Multimodal Large Language Models (MLLMs), yet their computational costs surge drastically when scaling resolution, training data, and model parameters. A key bottleneck stems from the proliferation of visual tokens required for fine-grained image understanding. We propose Skip-Vision, a unified framework addressing both training and inference inefficiencies in vision-language models. On top of conventional token compression approaches, our method introduces two complementary acceleration strategies. For training acceleration, we observe that Feed-Forward Network (FFN) computations on visual tokens induce marginal feature updates. This motivates our Skip-FFN strategy, which bypasses FFN layers for redundant visual tokens. For inference acceleration, we design a selective KV-cache removal mechanism that prunes the skipped key-value pairs during decoding while preserving model performance. Experimental results demonstrate that Skip-Vision reduces training time by up to 35%, inference FLOPs by 75%, and latency by 45%, while achieving comparable or superior performance to existing methods. Our work provides a practical solution for scaling high-performance MLLMs with enhanced efficiency.

1. Introduction

Transformer-based large-scale models have significantly advanced progress in Artificial Intelligence (AI) [10, 87, 102]. Their remarkable capabilities have driven the emergence of modern Multimodal Large Language Models (MLLMs) [2, 3, 69, 89], which demonstrate vision-

language competencies comparable to human performance. Empirical evidence suggests that scaling laws continue to be effective, primarily across three dimensions: visual scaling [40, 67, 112], data scaling [63, 64], and model scaling [56, 105]. However, these scaling methods present substantial efficiency issues, significantly increasing the training and inference burden. In a typical LLaVA-1.5 framework [69], where the model receives 576 visual tokens and 40 text tokens, inference using Vicuna-13B [24] LLM backbone demands 200 trillion FLOPS [42]. These motivate our pursuit of an MLLM architecture that optimally balances efficiency and performance.

Recent advances in Multimodal Large Language Models (MLLMs), such as Chain-of-Sight (CoS)[40] and LLaVA-Next[68], have improved performance by increasing visual tokens. However, during the Supervised Fine-Tuning (SFT) stage, the computational cost rises dramatically, leading to diminishing returns and making the scaling unsustainable. As shown in Figure 1, CoS requires a 165% increase in training resources and a 400% increase in inference computation for a mere 1.7% performance improvement, while LLaVA-Next faces similar inefficiencies. This challenge emphasizes the need to reduce visual token computation. Approaches like token compression or pruning [21, 39, 60, 109, 116, 119], while efficient, risk losing critical visual information, revealing a trade-off between efficiency and performance. This work aims to optimize the model’s computational efficiency from an architectural perspective, proposing a scalable solution that balances efficiency with visual fidelity.

We systematically examine the parameter count and FLOPs distribution across different components of the LLM. As shown in Table 1, using LLaMA-3 [28] as an ex-

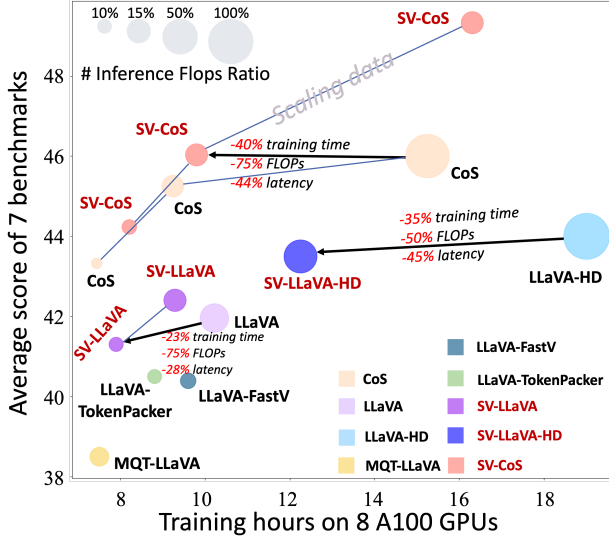


Figure 1. **Performance-efficiency trade-off curve.** Each circle denotes a model configuration, where our models utilize the Skip-Vision framework, with CoS [40], LLava-HD [67] and LLava [69] serving as baselines. Circle sizes reflect the inference FLOPs ratio. Skip-Vision demonstrate superior performance, scaling effectively with increased FLOPs and data and achieving higher inference efficiency when compared to baselines and other efficient MLLM methods. All methods utilize LLaMA3 8B as the foundational large language model.

Llama layer	Complexity	Parameters
FFN	$10.5LNC^2$	$5.64B(70\%)$
Attention	$2LN^2C + 1.5NC^2$	$1.34B(17\%)$
Embedding	-	$0.5B(6\%)$

Table 1. **Computational complexity and parameter statistics for Llama3 8B.** L denotes the number of blocks, N represents the number of input tokens, and C is the feature dimensionality

ample, the parameter and FLOPS requirements for the FFN component are significantly higher than those for the attention module. Furthermore, as illustrated in Figure 2, when the number of visual tokens is large, the majority of computations are concentrated on FFN of these tokens. In particular, we computed the difference in the magnitudes of the features before and after the FFN transformation for different tokens. As illustrated in the figure 3, we observe that the updates introduced by the FFN to the visual tokens are significantly smaller than those that affect the text tokens. This observation suggests a potential approach: **could we bypass FFN computations for a substantial portion of visual tokens?** Furthermore, in the autoregressive training framework of MLLMs, only the final visual token utilizes its last hidden state for next-token prediction, while the other visual tokens primarily serve to convey causal information. During model inference, inspired by [7], we observe that most visual information is progressively integrated into the final token through the early causal layers. This raises the possibility of reducing reliance on the full visual scaling KV cache throughout inference, potentially accelerating the inference process.

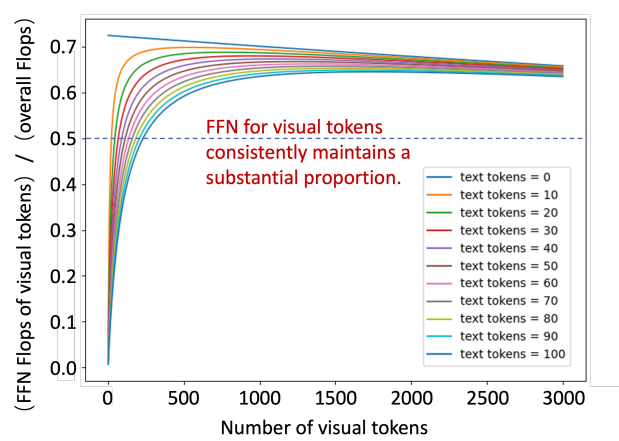


Figure 2. **Flops ratio of visual tokens in FFN.** When visual tokens greatly outnumber text tokens, computation is predominantly consumed by the FFN of visual tokens. Reducing their passage through the FFN can thus markedly decrease computational costs.

Building on these insights, we propose Skip-Vision, a novel and flexible architecture designed for more efficient scaling (see Figure 1 for a comparison). Visual tokens derived from smaller window/scale sizes constitute approximately 80% of the total visual tokens and account for most of the computational overhead. To mitigate this, as shown in Figure 4, we allow these tokens to skip the Feed-Forward Network (FFN) computation, significantly reducing overall computational costs. To address redundancy within skipped vision tokens, we can apply a token merging strategy for further simplification. During inference, skipped tokens are removed from the KV cache after the pre-fill phase, accelerating subsequent computation. Empirical results demonstrate that Skip-Vision reduces training time by up to 35%, FLOPs of inference by 75% and inference latency by 45%, while maintaining or even improving performance. These efficiency gains provide a scalable solution for large-scale multimodal learning, enabling better data utilization and enhanced model scalability.

In summary, our contributions are as follows.

- We introduce a novel and efficient Skip-Vision framework, using token merge and skip FFN strategy during training to reduce redundant computation for visual tokens.
- In inference, our framework employs a skip KV-cache mechanism that removes skip-FFN visual tokens from the KV-cache, enhancing efficiency.
- We present a theoretical analysis of the performance error in Skip-Vision and establish an error bound, which will be empirically validated through experiments.

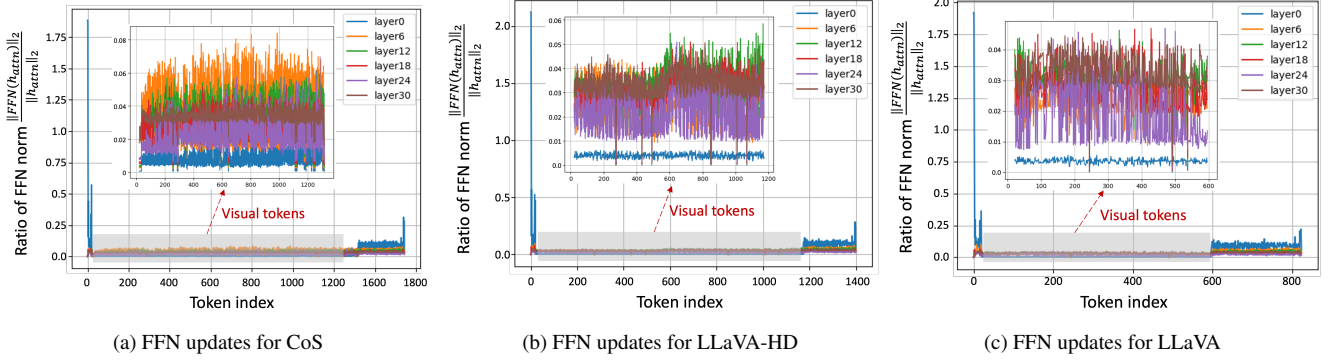


Figure 3. **FFN impact for different MLLMs.** We evaluate FFN impact by computing the feature modulus ratio before ($\|h_{\text{attn}}\|_2$) and after FFN ($\|\text{FFN}(h_{\text{attn}})\|_2$). The FFN introduces significantly smaller updates to visual tokens compared to text tokens.

- Experiments show our model’s superior efficiency, effective data scaling, and performance on par with state-of-the-art models of similar scale.

2. Related work

2.1. Vision-Language models

Rapid progress in large language models (LLMs) [24, 28, 114] has laid a solid foundation for the emergence of large-scale vision-language models (VLMs) [3, 6, 18, 58]. Flamingo [3] was a pioneering effort, integrating pre-trained image encoders with LLMs to handle multimodal data, thereby allowing comprehensive understanding and reasoning across modalities. Following this, the major models developed by leading corporations, such as GPT-4v [2] and Gemini-1.5-Pro [89], have led the progress in this domain. Using proprietary data sets and undisclosed training methodologies, these models have elevated multimodal intelligence to unprecedented levels.

At the same time, the open-source community has worked diligently to stay abreast of these advancements. The LLaVA series models [56, 67, 69, 112] exemplify a key strategy in this domain by mapping visual features directly into the input embedding space of the language model, integrating them as input tokens. However, this approach generates a substantial volume of visual tokens, frequently exceeding the number of text tokens, creating efficiency challenges. InternVL-1.5 [23] adopts dynamic high-resolution techniques, segmenting large images into smaller fragments for processing and scaling them accordingly. MiniCPM-V [117] utilizes a perceiver resampler structure with a single layer of cross-attention to compress visual tokens. Models such as Vary [108], SPHINX [64], Cambrian-1 [101], and BRAVE [47] leverage multi-visual encoder architectures to strengthen their visual processing capabilities. Furthermore, a crucial factor contributing to the effectiveness of modern VLMs is instruction fine-tuning [27, 67, 131], enabling these models to function as conversational agents and

interact with users through natural, human-like dialogue.

2.2. Efficient multimodal large language models

To enhance the efficiency of vision-language models, one of the primary and widely employed approaches in contemporary research involves reducing the size of the backbone models [26, 36, 83, 123, 130, 133]. Simultaneously, given that visual tokens contribute significantly to computational demands, research focused on compressing or refining these tokens has garnered increasing attention. Such methods are often coupled with the design of vision-language projectors. For instance, techniques like the Perceiver Resampler [3, 6, 41] and Q-Former [58] utilize transformer-based mechanisms to consolidate visual tokens into more compact query sets. In this way, the transformer outputs corresponding to the positions of the learnable latent queries serve as the aggregated representation of the visual features [42]. Honeybee [14] propose two visual projectors, namely C-Abstractor and D-Abstractor. LLaVA-PruMerge [92] and MADTP [12] introduce adaptive methods for reducing visual tokens. In addition, while the large language model (LLM) field has employed various techniques for token reduction to accelerate inference and compress KV cache [34, 128], research in this area remains limited within the MLLM domain.

3. Preliminaries

3.1. Decoder-only LLM

Each Transformer layer in a decoder-only LLM primarily consists of a self-attention layer and a feed-forward neural network. To facilitate autoregressive inference, the use of a KV-cache has been developed to accelerate the decoding process.

Self-Attention Mechanism: The self-attention mechanism enables each token in a sequence to selectively attend to other tokens, capturing contextual dependencies. Each token generates a query (Q), key (K), and value (V) vector.

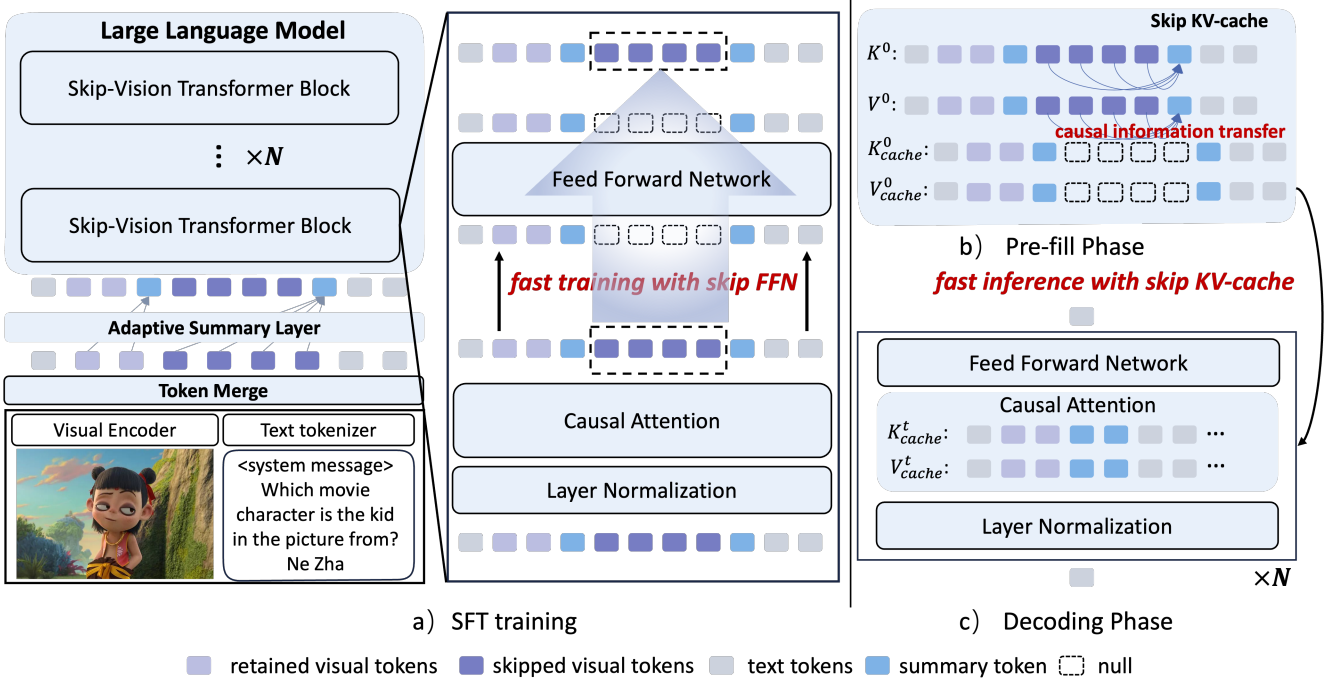


Figure 4. **The framework of Skip-Vision.** a) While visual scaling enriches visual information, it also increases computational overhead. Skip-Vision uses a skip-FFN strategy during training to reduce redundant computation for visual tokens. The numerous skipped tokens will be limited to the attention layer and bypass FFN. b) At the beginning of inference, Skip-Vision will remove skip-FFN visual tokens from the initial KV-cache, enhancing efficiency. c) During inference, skip attention leverages the skip KV-cache to accelerate generation.

Attention scores are calculated by the scaled dot-product:

$$\text{Attention}(Q, K, V) = \text{softmax} \left(\frac{QK^T}{\sqrt{d_k}} \right) V, \quad (1)$$

where d_k is the dimension of K . This formulation allows each token to incorporate information from others based on relevance, making self-attention critical in capturing relationships across tokens.

Feed-Forward Neural Network: The feed-forward neural network enhances token representations following the self-attention layer. The operation can be expressed as:

$$\text{FFN}(x) = \text{Activation}(xW_1 + b_1)W_2 + b_2, \quad (2)$$

where x is the input, W_1 and W_2 are weight matrices, and b_1 and b_2 are biases. This architecture allows the model to capture complex patterns and improve the expressiveness of token representations.

KV-cache: The key-value cache (KV-cache) stores key (K) and value (V) representations from previous self-attention computations, enabling efficient reuse during inference. This approach avoids redundant calculations for earlier tokens, improving inference speed.

The attention score is computed using $\text{Attention}(Q, K_{\text{cache}}^t, V_{\text{cache}}^t)$, where Q is the query for the current token. At each time step t , the cache is

updated as:

$$K_{\text{cache}}^{(t)} = [K_{\text{cache}}^{(t-1)}; K_t], \quad V_{\text{cache}}^{(t)} = [V_{\text{cache}}^{(t-1)}; V_t], \quad (3)$$

where K_t and V_t are the current token's key and value. This mechanism enhances computational efficiency and accelerates token generation.

4. Method

4.1. Skipped token selection and token merge

Before applying the skip FFN strategy, we first identify the skipped and retained visual tokens. The retained tokens should preserve most essential visual information, while the skipped tokens serve as complementary details, ensuring efficiency without significant loss of information.

Fortunately, in MLLM architectures, we can naturally distinguish retained and skipped tokens based on global and local context tokens. Global context tokens are retained, while local context tokens are skipped. In architectures like LLaVA-HD, global tokens originate from the resized full image, whereas local tokens come from smaller image patches. In CoS, global tokens correspond to larger window sizes, while local tokens are derived from smaller windows. Since LLaVA lacks a clear distinction between global and local tokens, inspired by [115], we select the top- n tokens

most similar to the CLS token as retained tokens, categorizing the rest as skipped tokens.

To further reduce the computational burden, it is necessary to refine the visual tokens to eliminate excessive redundancy. As shown in Figure 5, we conducted a similarity analysis of the visual tokens in CoS at different levels, calculating their similarity density. We found that the smaller the granularity of the visual tokens, the higher their average similarity, while their token count is significantly greater than that of other granularities. Consequently, inspired by ToMe [9], we employ a token merge method to reduce redundancy in skipped tokens, as detailed below:

- **Compute cosine similarities:** calculate the cosine similarity between each pair of tokens in the set, obtaining an average similarity score for each token.
- **Select top k distinctive Tokens:** sort tokens by average similarity in ascending order and retain the top k tokens with the lowest average similarity, representing the most distinctive information.
- **Merge remaining tokens:** for the remaining $n - k$ tokens, merge each one with the most similar token among the top k , thus consolidating information efficiently.

4.2. Training speed-up: skip FFN

As depicted in Figure 4a, we propose the FFN skip strategy: The retained visual tokens, which are few in number, proceed conventionally through all decoder layers of the LLM, while the numerous skipped visual tokens will be limited to the self-attention layers of each transformer block. For a given layer l , the output of retained tokens $h_{\text{retained}}^{(l)}$ is the sum of the self-attention output $h_{\text{attn}}^{(l)}$ and the FFN-transformed features $\text{FFN}^{(l)}(h_{\text{attn}}^{(l)})$:

$$h_{\text{retained}}^{(l)} = h_{\text{attn}}^{(l)} + \text{FFN}^{(l)}(h_{\text{attn}}^{(l)}). \quad (4)$$

The output of the skipped tokens is:

$$h_{\text{skipped}}^{(l)} = h_{\text{attn}}^{(l)}. \quad (5)$$

However, bypassing the FFN layers presents a non-trivial challenge. In the autoregressive training process, the final token of the vision sequence is used to predict the initial token of the text sequence, necessitating a specialized design for this terminal vision token. To facilitate this transition effectively, it must pass through the FFN layers, which are enriched with stored linguistic information [31, 84].

To address this, as shown in Figure 4, we introduce adaptive summary tokens to efficiently consolidate visual information. This token is generated by the Adaptive Summary Layer before the token sequence is input into the LLM. The layer comprises a simple linear transformation, and its computation is defined as follows:

$$x^s = (\text{softmax}(X \cdot W^T))^T \cdot X, \quad (6)$$

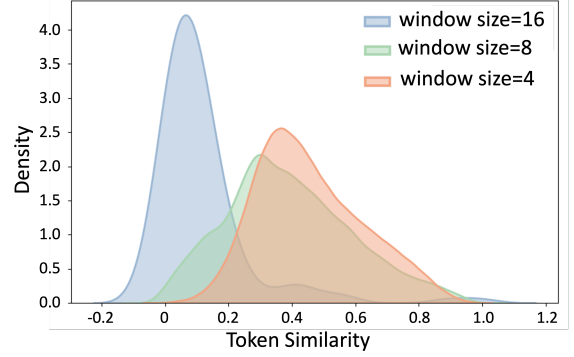


Figure 5. **Similarity density statistics.** We conducted a similarity density analysis in CoS, examining the visual tokens derived from various window scale. The results indicate that as the window scale decreases, the similarity between visual tokens becomes more pronounced, reflecting higher token redundancy.

where X denotes the retained or skipped visual tokens, $x^s \in \mathbb{R}^{1 \times C}$ is the summary token, and $W \in \mathbb{R}^{1 \times C}$ is the weight matrix. Leveraging this layer, we concatenate a summary token on both ends of the skipped visual tokens before their input to the LLM. The first summary token aggregates essential information from retained tokens, mitigating potential loss from extended token sequences. The second summary token integrates prior sequence information and plays a key role in predicting the next text token.

4.3. Inference speed-up: skip KV-cache

After training, our Skip-Vision framework incorporates skip KV-cache method to further improve efficiency:

$$K_{\text{skip-cache}}^{(0)} = K_{\text{cache}}^{(0)} \setminus K_{\text{skip}}, \quad V_{\text{skip-cache}}^{(0)} = V_{\text{cache}}^{(0)} \setminus V_{\text{skip}}, \quad (7)$$

As depicted in Figures 4 b) and c), given the autoregressive nature of LLMs, earlier token information is progressively transferred to later tokens. Skip FFN further enhances this integration by suppressing the attention weights of skipped tokens, forcing the model to focus on key tokens and improving information aggregation efficiency. Empirical results show that, due to the inclusion of summary tokens, this omission does not compromise model performance, underscoring a distinctive advantage of our framework for more efficient inference.

5. Theoretical analysis of Skip-Vision

At the core of this analysis lies the layer error incurred when bypassing the FFN layer. For a given layer l , the original output $h_{\text{original}}^{(l)}$ is: $h_{\text{original}}^{(l)} = h_{\text{attn}}^{(l)} + \text{FFN}^{(l)}(h_{\text{attn}}^{(l)})$. When skipping the FFN, the output becomes: $h_{\text{skip}}^{(l)} = h_{\text{attn}}^{(l)}$. The

per-layer skipping error is:

$$\epsilon^{(l)} = \|h_{\text{original}}^{(l)} - h_{\text{skip}}^{(l)}\|_2 = \|\text{FFN}^{(l)}(h_{\text{attn}}^{(l)})\|_2. \quad (8)$$

For redundant tokens, such as those in homogeneous image regions, this error is negligible ($\epsilon^{(l)} \approx 0$) due to minimal feature transformations by the FFN.

However, errors propagate through subsequent layers, amplified by the recursive nature of transformer architectures. Leveraging Lipschitz continuity assumptions for self-attention and FFN operations ($L_{\text{attn}}^{(l+1)}$ and $L_{\text{FFN}}^{(l+1)}$), the cumulative error at layer $l + 1$ is bounded by:

$$\epsilon^{(l+1)} \leq (L_{\text{attn}}^{(l+1)} + L_{\text{FFN}}^{(l+1)}) \cdot \epsilon^{(l)} + \epsilon_{\text{skip}}^{(l+1)}, \quad (9)$$

where ($\epsilon_{\text{skip}}^{(l+1)}$ represents new errors from skipping deeper layers $(l + 1)$).

Over L layers, the total error telescopes to:

$$\epsilon_{\text{total}} \leq \sum_{l=1}^L \epsilon_{\text{skip}}^{(l)} \cdot \prod_{i=1}^{L-l} (L_{\text{attn}}^{(i+1)} + L_{\text{FFN}}^{(i+1)}). \quad (10)$$

Theorem 5.1 Bounded Lipschitz. *If W_Q, W_K, W_V, W_1, W_2 are orthogonal matrices (spectral norm = 1), then:*

- $L(\text{attn}) \leq 1/\sqrt{d_k}$
- $L(\text{FFN}) \leq 1$

Follow Theorem 5.1, we assume Lipschitz constants $L_{\text{attn}} + L_{\text{FFN}} \leq \gamma$ and skipping errors $\epsilon_{\text{skip}}^{(l)} \leq \epsilon$, the total error is scaled to:

$$\epsilon_{\text{total}} \leq \epsilon \cdot \frac{\gamma^L - 1}{\gamma - 1}, \quad (11)$$

Equation 11 establishes that the skip error is bounded when $\gamma < 1$, provided the model is trained with modern regularization techniques. This ensures that the MLLM remains less sensitive to the effects of skipping.

This error also impacts the KL divergence between the original and skipped outputs, bounded by:

$$\mathcal{D}_{\text{KL}}(p_{\text{skip}} \parallel p_{\text{original}}) \leq \frac{1}{2\sigma^2} \cdot \epsilon_{\text{total}}^2, \quad (12)$$

where σ^2 is the variance of the logits. Further integrating feature similarity errors ($\epsilon_{\text{sim}} = O(\sqrt{1-\theta})$) from low-attention tokens, the final bound becomes:

$$\mathcal{D}_{\text{KL}} \leq \frac{1}{2\sigma^2} \cdot (\epsilon_{\text{total}} + \epsilon_{\text{sim}})^2. \quad (13)$$

Practically, this analysis motivates a layer-wise skipping strategy, alongside token selection and merge based on feature similarity (θ). **More analysis and the proof of Theorem 5.1 are provided in the Appendix.**

6. Experiments

6.1. Benchmarks

To comprehensively evaluate our model, we conducted experiments on eight different benchmarks. These include MME [29], which assesses the perceptual and cognitive capabilities of multimodal language models; TextVQA [96], focused on fine-grained visual question answering; MM-Bench [72] and MMStar [20] for general diagnostic capabilities; MMMU [124], designed to test STEM-related reasoning; MathVista [76], which evaluates mathematical problem solving skills; OCRBench [70], for optical character recognition tasks; and MMVet [121], used for subjective assessment. Taken together, these benchmarks offer a comprehensive framework for assessing the efficacy of the model in various multimodal challenges.

6.2. Efficiency evaluation

We systematically evaluate both training time (*hours*), inference FLOP computation and inference latency (*ms*) on single A100 GPU. For training efficiency, we report actual GPU hours measured on consistent hardware configurations. For inference FLOPs, we adopt the methodology from FastV [21], specifically tracking the computational demands of processing visual tokens. In the LLama architecture, we calculate FLOPs for the causal attention and feed forward network modules as $4NC^2 + 2N^2C + 3NCM$ where N is the token count, C denotes the hidden state dimension, and M is the intermediate FFN dimension. Skip-Vision framework adjusts token counts dynamically between the attention and FFN modules, allowing us to refine FLOP calculations as $4N_1C^2 + 2N_1^2C + 3N_2CM$, where N_1 and N_2 represent the visual token counts processed in the causal attention and FFN layers, respectively.

6.3. Data setup

During pretraining, we adopt the experimental settings of LLava and CoS, utilizing LLava-558K [69] and 65 million image-text pairs for respective comparisons. For the Supervised Fine-Tuning phase, we use LLava-665K [69] for all comparative experiments. By leveraging the computational efficiency of Skip-Vision framework, the resources saved can be redirected toward scaling the dataset to further enhance model performance. To this end, we extend our dataset to SV-1M, comprising 1 million samples, demonstrating the substantial performance improvements achievable through data expansion. To further assess our approach against state-of-the-art models of similar scale, we extend the dataset to SV-9M, underscoring the scalability and potential of our method. Detailed dataset statistics are provided in the Appendix.

	MME	Textvqa	MMB	MMVet	MMMU	MathV	OCRB	MMStar	Avg	Hours	FLOPs	Latency
LLaVA setting:												
LLaVA [69]	1535	58.6	72.2	32.8	39.6	21.3	32.7	36.5	42.0	10.2	100%	125
LLaVA-FastV [21]	1453	56.1	71	32.4	37.3	20.6	28.8	36.3	40.4	9.6	30%	103
MQT-LLaVA [39]	1487	53.6	69	28.2	37.8	16.8	28.1	36.5	38.6	7.5	44%	106
LLaVA-Tokenpacker [60]	1538	56.2	72.3	32.1	39.0	19.3	29.8	35.0	40.5	8.8	24%	97
SV-LLaVA	1519	56.5	72.5	32.4	38.8	21.2	30.7	36.5	41.3	7.9	25%	90
$(N_r = 100, N_s = 156)$	-1%	-3.6%	$+0.4\%$	-1.2%	-2%	-0.5%	-3.6%	-6.1%	-1.7%	-22.5%	-75%	-28%
SV-LLaVA	1530	57.3	72.7	35.6	39.2	21.4	32.0	40.0	42.6	9.0	60%	103
$(N_r = 256, N_s = 316)$	-0.3%	-2.2%	$+0.7\%$	$+8.5\%$	-1%	$+0.5\%$	-2.1%	$+9.6\%$	$+1.4\%$	-11.8%	-40%	-17.6%
LLaVA-HD setting:												
LLaVA-HD [67]	1533	64	71.8	35.3	39.3	20	37.4	40.5	44.0	19	100%	450
SV-LLaVA-HD	1534	61.2	73.1	35.9	39.7	21.2	34.1	39.3	43.5	12.2	50%	250
$(N_r = 576, N_s = 576)$	$+0\%$	-4.3%	$+1.8\%$	$+1.7\%$	$+1.5\%$	-6%	-8.8%	-2.9%	-1.1%	-35.8%	-50%	-44.4%
CoS setting:												
CoS [40]	1585	64.4	77.1	39.4	39.2	21.5	39.2	41.2	46.0	15.3	100%	160
SV-CoS	1563	63.7	76.5	41.7	40.3	21.2	37	41.9	46.0	9.8	25%	90
$(N_r = 272, N_s = 256)$	-1.4%	-1.1%	-0.8%	$+5.8\%$	$+2.8\%$	-1.4%	-5.6%	$+1.7\%$	-0%	-40%	-75%	-43.8%
SV-CoS (SV-1M)	1569	67.1	77.1	43.3	40.7	22.0	50.7	44.4	49.3	16.3	25%	90

Table 2. **Performance and efficiency evaluation.** We evaluate Skip-Vision on LLaVA, LLaVA-HD, and CoS and compare it with state-of-the-art efficiency optimization models under the LLaVA setting. N_r and N_s denote the number of retained and skipped tokens, respectively.

	LLM	MME	Textvqa	MMB	MMVet	MMMU	MathV	OCRB	MMStar
Open-source models in 8B tier:									
mPLUG-Owl3 [118]	Qwen2	-	69.0	<u>77.6</u>	40.1	-	65.0	-	40.1
Cambrian [101]	LLaMA3	1547	<u>71.7</u>	75.9	-	42.7	49.0	62.4	-
LLaVA [69]	LLaMA3	1535	58.6	72.2	32.8	39.6	21.3	32.7	36.5
Mini-Gemini-HD [61]	LLaMA3	1606	70.2	72.7	-	37.3	37.0	47.7	-
LLaVA-Next [56]	LLaMa3	<u>1604</u>	64.6	72.1	-	41.7	36.3	49.0	-
Ovis [77]	LLaMA3	-	-	77.4	-	<u>44.7</u>	40.8	-	<u>49.5</u>
MiniCPM-V2.5 [117]	LLaMA3	-	76.6	77.6	-	45.8	54.3	72.5	-
SV-CoS (SV-9M)	LLaMA3	1550	69.1	78.4	51.7	43	<u>61.3</u>	<u>69.4</u>	52.3

Table 3. **MLLM evaluation.** We present the performance of SV-CoS on SV-9M, comparing it against the current SOTA models of a similar scale. The highest scores are highlighted in **bold**, while the second-highest scores are indicated with underlines.

6.4. Training setup

For LLaVA and LLaVA-HD setting, we use input resolutions of 336 and a dynamic resolution ranging from 336 to 672, respectively, with CLIP ViT-L/336px [87] as the vision encoder and LLaMA3 8B Instruct [28] as the backbone. For CoS setting, pretraining is conducted at 224 resolution, training only the multi-scale visual resampler with CLIP ViT-L/224px [87]. The model processes 80 visual tokens, including 16 global and 64 local tokens, and scales to 336 and 1296 tokens during SFT. In SFT, the resolution increases to 448, and all model parameters are unfrozen for full optimization.

In all experiments, we used a learning rate of $1e^{-3}$ for pre-training, which is reduced to $1e^{-5}$ during SFT. Training follows a cosine decay schedule after a 3% warm-up phase. For skipped token selection, unless otherwise specified, the LLaVA setting includes 156 skipped tokens and

100 retained tokens, the LLaVA-HD setting has 576 skipped and 576 retained tokens, and the CoS setting consists of 256 skipped and 272 retained tokens. All skipped tokens undergo a token merging process to enhance efficiency.

6.5. Main experimental results

Performance and efficiency. We first evaluate the effectiveness of Skip-Vision across three different frameworks: CoS, LLaVA, and LLaVA-HD, demonstrating its ability to maximize efficiency while minimizing performance degradation. As shown in Figure 1 and Table 5, Skip-Vision reduces training time by 22.5%, inference FLOPs by 75%, and inference latency by 28% for LLaVA. For LLaVA-HD, it achieves a 35.8% reduction in training time, 50% in inference FLOPs, and 45% in inference latency. In CoS, it reduces training time by 35.8%, inference FLOPs by 75%, and inference latency by 44%.

Scaling. We evaluated the scalability of Skip-Vision,

	MME	Textvqa	MMB	MMVet	MMMU	MathV	OCRB	MMStar	Avg	Latency
SV-LLaVA (w/o SK)	1519	56.7	72.5	31.4	38.8	21.2	30.9	36.5	41.1	103
SV-LLaVA	1519	56.5	72.5	32.4	38.8	21.2	30.7	36.5	41.3	90
+0%	-0.4%	+0%	+3.2%	+0%	+0%	-0.6%	+0%	+0.5%	+0.5%	-9.7%
SV-LLaVA-HD (w/o SK)	1533	61.6	73.0	35.8	39.9	21.2	34.5	39.7	43.7	310
SV-LLaVA-HD	1534	61.2	73.1	35.9	39.7	21.2	34.1	39.3	43.5	250
+0%	-0.7%	+0.1%	+0.3%	-0.5%	+0%	-1.2%	-1%	-0.5%	-0.5%	-19.4%
SV-LLaVA-CoS (w/o SK)	1562	63.9	76.5	40.2	40.2	21.2	37.2	41.9	45.9	126
SV-LLaVA-CoS	1563	63.7	76.5	41.7	40.3	21.2	37	41.9	46.0	90
+0%	-0.3%	+0%	+3.7%	+0.2%	+0%	-0.5%	+0%	+0.2%	+0.2%	-28.6%

Table 4. **Ablation on skip KV-cache.** We evaluate SK (using skip KV-cache during inference) of Skip-Vision on different settings.

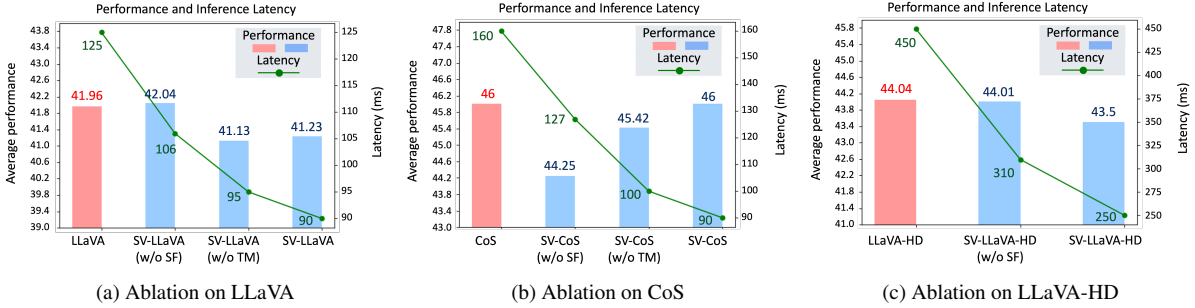


Figure 6. **Ablation study.** We performed an ablation study on each component of the Skip-Vision. SF (skip FFN), TM (token merge).

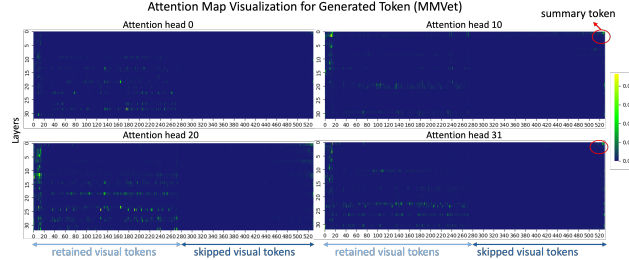


Figure 7. **Visualization of attention map in MMVet.**

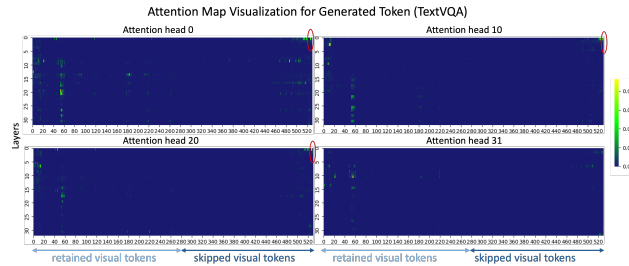


Figure 8. **Visualization of attention map in TextVQA.**

leveraging CoS’s visual scaling to increase visual tokens from 336 to 1296 while maintaining efficiency. Expanding the fine-tuning dataset from LLaVA-665k to SV-1M further improved performance by 8% over CoS_{1296} with similar resources. To benchmark against state-of-the-art models, we scaled to SV-9M, with training completed in 72 hours on 16 NVIDIA A100 GPUs (Table 3).

6.6. Ablation study and analysis

To validate the effectiveness of each component within the Skip-Vision framework, we conducted ablation and comparative experiments on token merge, skip FFN, and skip KV-cache.

As shown in Figure 6, both the skip FFN strategy and token merging enhance computational efficiency across different model settings while maintaining performance. Notably, skip FFN performs better in the CoS setting than in LLaVA and LLaVA-HD. We attribute this to CoS allowing the vision backbone to be fine-tuned during the SFT stage, enabling key information to be more effectively captured by summary tokens, thereby reducing the errors introduced by skip FFN. As shown in Table 4, skip KV-cache slightly affects fine-grained tasks such as TextVQA and OCRBench but improves performance in long-form response tasks like MMVet.

To further analyze this, we visualized attention maps across layers for visual tokens in SV-CoS during the MMVet and TextVQA tasks. In MMVet (Figure 7), the attention of generated tokens primarily focuses on retained and summary tokens, with skip KV-cache filtering out unnecessary noise. In TextVQA (Figure 8), which requires fine-grained understanding, attention is spread across both retained and skipped tokens, leading to some performance loss with skip KV-cache. However, causal attention effectively aggregates information from skipped tokens into the final summary tokens, allowing us to retain only the summary tokens and

retained visual tokens in the KV-cache.

7. Conclusion

We propose Skip-Vision, an efficient multimodal large language model architecture that boosts computational efficiency through a skip-FFN strategy, reducing redundant computations over visual tokens during training. During inference, Skip-Vision uses a skip KV-cache to accelerate processing by omitting non-essential visual tokens from the KV cache. Extensive experiments show our model outperforms current methods in efficiency and scales effectively with data, delivering competitive performance among leading models of similar scale.

References

- [1] Manoj Acharya, Kushal Kafle, and Christopher Kanan. Tallyqa: Answering complex counting questions. In *Proceedings of the AAAI conference on artificial intelligence*, pages 8076–8084, 2019. 5
- [2] Josh Achiam, Steven Adler, Sandhini Agarwal, Lama Ahmad, Ilge Akkaya, Florencia Leoni Aleman, Diogo Almeida, Janko Altenschmidt, Sam Altman, Shyamal Anadkat, et al. Gpt-4 technical report. *arXiv preprint arXiv:2303.08774*, 2023. 1, 3
- [3] Jean-Baptiste Alayrac, Jeff Donahue, Pauline Luc, Antoine Miech, Iain Barr, Yana Hasson, Karel Lenc, Arthur Mensch, Katherine Millican, Malcolm Reynolds, et al. Flamingo: a visual language model for few-shot learning. *Advances in neural information processing systems*, 35: 23716–23736, 2022. 1, 3
- [4] Stanislaw Antol, Aishwarya Agrawal, Jiasen Lu, Margaret Mitchell, Dhruv Batra, C Lawrence Zitnick, and Devi Parikh. Vqa: Visual question answering. In *Proceedings of the IEEE international conference on computer vision*, pages 2425–2433, 2015. 5
- [5] Gilles Baechler, Srinivas Sunkara, Maria Wang, Fedir Zubach, Hassan Mansoor, Vincent Etter, Victor Cărbune, Jason Lin, Jindong Chen, and Abhanshu Sharma. Screenai: A vision-language model for ui and infographics understanding. *arXiv preprint arXiv:2402.04615*, 2024. 5
- [6] Jinze Bai, Shuai Bai, Shusheng Yang, Shijie Wang, Sinan Tan, Peng Wang, Junyang Lin, Chang Zhou, and Jingren Zhou. Qwen-vl: A versatile vision-language model for understanding, localization, text reading, and beyond. *arXiv preprint arXiv:2308.12966*, 1(2):3, 2023. 3
- [7] Samyadeep Basu, Martin Grayson, Cecily Morrison, Bessmira Nushi, Soheil Feizi, and Daniela Massiceti. Understanding information storage and transfer in multi-modal large language models. *arXiv preprint arXiv:2406.04236*, 2024. 2
- [8] Ali Furkan Biten, Ruben Tito, Andres Mafla, Lluis Gomez, Marçal Rusinol, Ernest Valveny, CV Jawahar, and Dimosthenis Karatzas. Scene text visual question answering. In *Proceedings of the IEEE/CVF international conference on computer vision*, pages 4291–4301, 2019. 5
- [9] Daniel Bolya, Cheng-Yang Fu, Xiaoliang Dai, Peizhao Zhang, Christoph Feichtenhofer, and Judy Hoffman. Token merging: Your vit but faster. *arXiv preprint arXiv:2210.09461*, 2022. 5
- [10] Tom B Brown. Language models are few-shot learners. *arXiv preprint arXiv:2005.14165*, 2020. 1
- [11] Shihao Cai, Keqin Bao, Hangyu Guo, Jizhi Zhang, Jun Song, and Bo Zheng. Geopt4v: Towards geometric multimodal large language models with geometric image generation. *arXiv preprint arXiv:2406.11503*, 2024. 5
- [12] Jianjian Cao, Peng Ye, Shengze Li, Chong Yu, Yansong Tang, Jiwen Lu, and Tao Chen. Madtp: Multimodal alignment-guided dynamic token pruning for accelerating vision-language transformer. In *Proceedings of the IEEE/CVF Conference on Computer Vision and Pattern Recognition*, pages 15710–15719, 2024. 3
- [13] Jimmy Carter. Textocr-gpt4v. <https://huggingface.co/datasets/jimmycarter/textocr-gpt4v>, 2024. 5
- [14] Junbum Cha, Wooyoung Kang, Jonghwan Mun, and Byungseok Roh. Honeybee: Locality-enhanced projector for multimodal llm. In *Proceedings of the IEEE/CVF Conference on Computer Vision and Pattern Recognition*, pages 13817–13827, 2024. 3
- [15] Chungkwong Chan. Stroke extraction for offline handwritten mathematical expression recognition. *IEEE Access*, 8: 61565–61575, 2020. 5
- [16] Shuaichen Chang, David Palzer, Jialin Li, Eric Fosler-Lussier, and Ningchuan Xiao. Mapqa: A dataset for question answering on choropleth maps. *arXiv preprint arXiv:2211.08545*, 2022. 5
- [17] Guiming Hardy Chen, Shunian Chen, Ruifei Zhang, Junying Chen, Xiangbo Wu, Zhiyi Zhang, Zhihong Chen, Jianquan Li, Xiang Wan, and Benyou Wang. Allava: Harnessing gpt4v-synthesized data for a lite vision-language model, 2024. 5
- [18] Keqin Chen, Zhao Zhang, Weili Zeng, Richong Zhang, Feng Zhu, and Rui Zhao. Shikra: Unleashing multimodal llm’s referential dialogue magic. *arXiv preprint arXiv:2306.15195*, 2023. 3
- [19] Lin Chen, Jisong Li, Xiaoyi Dong, Pan Zhang, Conghui He, Jiaqi Wang, Feng Zhao, and Dahua Lin. Sharegpt4v: Improving large multi-modal models with better captions. *arXiv preprint arXiv:2311.12793*, 2023. 5
- [20] Lin Chen, Jinsong Li, Xiaoyi Dong, Pan Zhang, Yuhang Zang, Zehui Chen, Haodong Duan, Jiaqi Wang, Yu Qiao, Dahua Lin, et al. Are we on the right way for evaluating large vision-language models? *arXiv preprint arXiv:2403.20330*, 2024. 6
- [21] Liang Chen, Haozhe Zhao, Tianyu Liu, Shuai Bai, Junyang Lin, Chang Zhou, and Baobao Chang. An image is worth 1/2 tokens after layer 2: Plug-and-play inference acceleration for large vision-language models. *arXiv preprint arXiv:2403.06764*, 2024. 1, 6, 7, 2
- [22] Xingyu Chen, Zihan Zhao, Lu Chen, Danyang Zhang, Jiaabao Ji, Ao Luo, Yuxuan Xiong, and Kai Yu. Websrc: A dataset for web-based structural reading comprehension. *arXiv preprint arXiv:2101.09465*, 2021. 5

[23] Zhe Chen, Weiyun Wang, Hao Tian, Shenglong Ye, Zhang-wei Gao, Erfei Cui, Wenwen Tong, Kongzhi Hu, Jiapeng Luo, Zheng Ma, et al. How far are we to gpt-4v? closing the gap to commercial multimodal models with open-source suites. *arXiv preprint arXiv:2404.16821*, 2024. 3

[24] Wei-Lin Chiang, Zhuohan Li, Zi Lin, Ying Sheng, Zhang-hao Wu, Hao Zhang, Lianmin Zheng, Siyuan Zhuang, Yonghao Zhuang, Joseph E. Gonzalez, Ion Stoica, and Eric P. Xing. Vicuna: An open-source chatbot impressing gpt-4 with 90%* chatgpt quality. <https://lmsys.org/blog/2023-03-30-vicuna/>, 2023. 1, 3

[25] Chee Kheng Chng, Yuliang Liu, Yipeng Sun, Chun Chet Ng, Canjie Luo, Zihan Ni, ChuanMing Fang, Shuaítao Zhang, Junyu Han, Errui Ding, et al. Icdar2019 robust reading challenge on arbitrary-shaped text-rrc-art. In *2019 International Conference on Document Analysis and Recognition (ICDAR)*, pages 1571–1576. IEEE, 2019. 5

[26] Xiangxiang Chu, Limeng Qiao, Xinyang Lin, Shuang Xu, Yang Yang, Yiming Hu, Fei Wei, Xinyu Zhang, Bo Zhang, Xiaolin Wei, et al. Mobilevlm: A fast, reproducible and strong vision language assistant for mobile devices. *arXiv preprint arXiv:2312.16886*, 2023. 3

[27] Wenliang Dai, Junnan Li, Dongxu Li, Anthony Tiong, Junqi Zhao, Weisheng Wang, Boyang Li, Pascale Fung, and Steven Hoi. InstructBLIP: Towards general-purpose vision-language models with instruction tuning. In *Thirty-seventh Conference on Neural Information Processing Systems*, 2023. 3

[28] Abhimanyu Dubey, Abhinav Jauhri, Abhinav Pandey, Abhishek Kadian, Ahmad Al-Dahle, Aiesha Letman, Akhil Mathur, Alan Schelten, Amy Yang, Angela Fan, et al. The llama 3 herd of models. *arXiv preprint arXiv:2407.21783*, 2024. 1, 3, 7

[29] Chaoyou Fu, Peixian Chen, Yunhang Shen, Yulei Qin, Mengdan Zhang, Xu Lin, Jinrui Yang, Xiawu Zheng, Ke Li, Xing Sun, Yunsheng Wu, and Rongrong Ji. Mme: A comprehensive evaluation benchmark for multimodal large language models. *arXiv preprint arXiv:2306.13394*, 2024. 6

[30] Jiahui Gao, Renjie Pi, Jipeng Zhang, Jiacheng Ye, Wan-jun Zhong, Yufei Wang, Lanqing Hong, Jianhua Han, Hang Xu, Zhenguo Li, et al. G-llava: Solving geometric problem with multi-modal large language model. *arXiv preprint arXiv:2312.11370*, 2023. 5

[31] Mor Geva, Jasmijn Bastings, Katja Filippova, and Amir Globerson. Dissecting recall of factual associations in auto-regressive language models. *arXiv preprint arXiv:2304.14767*, 2023. 5

[32] Ankush Gupta, Andrea Vedaldi, and Andrew Zisserman. Synthetic data for text localisation in natural images. In *Proceedings of the IEEE conference on computer vision and pattern recognition*, pages 2315–2324, 2016. 5

[33] Danna Gurari, Qing Li, Chi Lin, Yinan Zhao, Anhong Guo, Abigale Stangl, and Jeffrey P Bigham. Vizwiz-priv: A dataset for recognizing the presence and purpose of private visual information in images taken by blind people. In *Proceedings of the IEEE/CVF Conference on Computer Vision and Pattern Recognition*, pages 939–948, 2019. 5

[34] Chi Han, Qifan Wang, Hao Peng, Wenhan Xiong, Yu Chen, Heng Ji, and Sinong Wang. Lm-infinite: Zero-shot extreme length generalization for large language models. In *Proceedings of the 2024 Conference of the North American Chapter of the Association for Computational Linguistics: Human Language Technologies (Volume 1: Long Papers)*, pages 3991–4008, 2024. 3

[35] Mengchao He, Yuliang Liu, Zhibo Yang, Sheng Zhang, Canjie Luo, Feiyu Gao, Qi Zheng, Yongpan Wang, Xin Zhang, and Lianwen Jin. Icpr2018 contest on robust reading for multi-type web images. In *2018 24th international conference on pattern recognition (ICPR)*, pages 7–12. IEEE, 2018. 5

[36] Muyang He, Yexin Liu, Boya Wu, Jianhao Yuan, Yueze Wang, Tiejun Huang, and Bo Zhao. Efficient multimodal learning from data-centric perspective. *arXiv preprint arXiv:2402.11530*, 2024. 3

[37] Anwen Hu, Haiyang Xu, Jiabo Ye, Ming Yan, Liang Zhang, Bo Zhang, Chen Li, Ji Zhang, Qin Jin, Fei Huang, et al. mplug-docowl 1.5: Unified structure learning for ocr-free document understanding. *arXiv preprint arXiv:2403.12895*, 2024. 5

[38] Anwen Hu, Haiyang Xu, Liang Zhang, Jiabo Ye, Ming Yan, Ji Zhang, Qin Jin, Fei Huang, and Jingren Zhou. mplug-docowl2: High-resolution compressing for ocr-free multi-page document understanding. *arXiv preprint arXiv:2409.03420*, 2024. 5

[39] Wenbo Hu, Zi-Yi Dou, Liunian Harold Li, Amita Kammath, Nanyun Peng, and Kai-Wei Chang. Matryoshka query transformer for large vision-language models. *arXiv preprint arXiv:2405.19315*, 2024. 1, 7

[40] Ziyuan Huang, Kaixiang Ji, Biao Gong, Zhiwu Qing, Qingsheng Zhang, Kecheng Zheng, Jian Wang, Jingdong Chen, and Ming Yang. Accelerating pre-training of multimodal llms via chain-of-sight. *arXiv preprint arXiv:2407.15819*, 2024. 1, 2, 7

[41] Andrew Jaegle, Felix Gimeno, Andy Brock, Oriol Vinyals, Andrew Zisserman, and Joao Carreira. Perceiver: General perception with iterative attention. In *International conference on machine learning*, pages 4651–4664. PMLR, 2021. 3

[42] Yizhang Jin, Jian Li, Yexin Liu, Tianjun Gu, Kai Wu, Zhengkai Jiang, Muyang He, Bo Zhao, Xin Tan, Zhenye Gan, et al. Efficient multimodal large language models: A survey. *arXiv preprint arXiv:2405.10739*, 2024. 1, 3

[43] Justin Johnson, Bharath Hariharan, Laurens Van Der Maaten, Li Fei-Fei, C Lawrence Zitnick, and Ross Girshick. Clevr: A diagnostic dataset for compositional language and elementary visual reasoning. In *Proceedings of the IEEE conference on computer vision and pattern recognition*, pages 2901–2910, 2017. 5

[44] Kushal Kafle, Brian Price, Scott Cohen, and Christopher Kanan. Dvqa: Understanding data visualizations via question answering. In *Proceedings of the IEEE conference on computer vision and pattern recognition*, pages 5648–5656, 2018. 5

[45] Samira Ebrahimi Kahou, Vincent Michalski, Adam Atkinson, Ákos Kádár, Adam Trischler, and Yoshua Bengio. Fig-

ureqa: An annotated figure dataset for visual reasoning. *arXiv preprint arXiv:1710.07300*, 2017. 5

[46] Shankar Kantharaj, Rixie Tiffany Ko Leong, Xiang Lin, Ahmed Masry, Megh Thakkar, Enamul Hoque, and Shafiq Joty. Chart-to-text: A large-scale benchmark for chart summarization. *arXiv preprint arXiv:2203.06486*, 2022. 5

[47] Oğuzhan Fatih Kar, Alessio Tonioni, Petra Poklukar, Achin Kulshrestha, Amir Zamir, and Federico Tombari. Brave: Broadening the visual encoding of vision-language models. *arXiv preprint arXiv:2404.07204*, 2024. 3

[48] Dimosthenis Karatzas, Lluís Gomez-Bigorda, Angelos Nicolaou, Suman Ghosh, Andrew Bagdanov, Masakazu Iwamura, Jiri Matas, Lukas Neumann, Vijay Ramaseshan Chandrasekhar, Shijian Lu, et al. Icdar 2015 competition on robust reading. In *2015 13th international conference on document analysis and recognition (ICDAR)*, pages 1156–1160. IEEE, 2015. 5

[49] Aniruddha Kembhavi, Mike Salvato, Eric Kolve, Minjoon Seo, Hannaneh Hajishirzi, and Ali Farhadi. A diagram is worth a dozen images. In *Computer Vision–ECCV 2016: 14th European Conference, Amsterdam, The Netherlands, October 11–14, 2016, Proceedings, Part IV* 14, pages 235–251. Springer, 2016. 5

[50] Aniruddha Kembhavi, Minjoon Seo, Dustin Schwenk, Jonghyun Choi, Ali Farhadi, and Hannaneh Hajishirzi. Are you smarter than a sixth grader? textbook question answering for multimodal machine comprehension. In *Proceedings of the IEEE Conference on Computer Vision and Pattern recognition*, pages 4999–5007, 2017. 5

[51] Sunjun Kweon, Yeonsu Kwon, Seonhee Cho, Yohan Jo, and Edward Choi. Open-wikititable: Dataset for open domain question answering with complex reasoning over table. *arXiv preprint arXiv:2305.07288*, 2023. 5

[52] Jason J Lau, Soumya Gayen, Asma Ben Abacha, and Dina Demner-Fushman. A dataset of clinically generated visual questions and answers about radiology images. *Scientific data*, 5(1):1–10, 2018. 5

[53] Hugo Laurençon, Andrés Marafioti, Victor Sanh, and Léo Tronchon. Building and better understanding vision-language models: insights and future directions., 2024. 5

[54] Seongyun Lee, Sue Hyun Park, Yongrae Jo, and Minjoon Seo. Volcano: mitigating multimodal hallucination through self-feedback guided revision. *arXiv preprint arXiv:2311.07362*, 2023. 5

[55] Paul Lerner, Olivier Ferret, Camille Guinaudeau, Hervé Le Borgne, Romaric Besançon, José G Moreno, and Jesús Lovón Melgarejo. Viquae, a dataset for knowledge-based visual question answering about named entities. In *Proceedings of the 45th International ACM SIGIR Conference on Research and Development in Information Retrieval*, pages 3108–3120, 2022. 5

[56] Bo Li, Kaichen Zhang, Hao Zhang, Dong Guo, Renrui Zhang, Feng Li, Yuanhan Zhang, Ziwei Liu, and Chunyuan Li. Llava-next: Stronger llms supercharge multimodal capabilities in the wild. <https://llava-vl.github.io/blog/2024-05-10-llava-next-stronger-llms/>, 2024. 1, 3, 7

[57] Bo Li, Yuanhan Zhang, Dong Guo, Renrui Zhang, Feng Li, Hao Zhang, Kaichen Zhang, Peiyuan Zhang, Yanwei Li, Ziwei Liu, et al. Llava-onevision: Easy visual task transfer. *arXiv preprint arXiv:2408.03326*, 2024. 5

[58] Junnan Li, Dongxu Li, Silvio Savarese, and Steven Hoi. Blip-2: Bootstrapping language-image pre-training with frozen image encoders and large language models. In *International conference on machine learning*, pages 19730–19742. PMLR, 2023. 3

[59] Lei Li, Yuqi Wang, Runxin Xu, Peiyi Wang, Xiachong Feng, Lingpeng Kong, and Qi Liu. Multimodal ArXiv: A dataset for improving scientific comprehension of large vision-language models. In *Proceedings of the 62nd Annual Meeting of the Association for Computational Linguistics (Volume 1: Long Papers)*, pages 14369–14387, Bangkok, Thailand, 2024. Association for Computational Linguistics. 5

[60] Wentong Li, Yuqian Yuan, Jian Liu, Dongqi Tang, Song Wang, Jie Qin, Jianke Zhu, and Lei Zhang. Tokenpacker: Efficient visual projector for multimodal llm. *arXiv preprint arXiv:2407.02392*, 2024. 1, 7

[61] Yanwei Li, Yuechen Zhang, Chengyao Wang, Zhisheng Zhong, Yixin Chen, Ruihang Chu, Shaoteng Liu, and Jiaya Jia. Mini-gemini: Mining the potential of multi-modality vision language models. *arXiv preprint arXiv:2403.18814*, 2024. 7

[62] Zhuowan Li, Xingrui Wang, Elias Stengel-Eskin, Adam Kortylewski, Wufei Ma, Benjamin Van Durme, and Alan L Yuille. Super-clevr: A virtual benchmark to diagnose domain robustness in visual reasoning. In *Proceedings of the IEEE/CVF Conference on Computer Vision and Pattern Recognition*, pages 14963–14973, 2023. 5

[63] Ji Lin, Hongxu Yin, Wei Ping, Pavlo Molchanov, Mohammad Shoeybi, and Song Han. Vila: On pre-training for visual language models. In *Proceedings of the IEEE/CVF Conference on Computer Vision and Pattern Recognition*, pages 26689–26699, 2024. 1

[64] Dongyang Liu, Renrui Zhang, Longtian Qiu, Siyuan Huang, Weifeng Lin, Shitian Zhao, Shijie Geng, Ziyi Lin, Peng Jin, Kaipeng Zhang, et al. Sphinx-x: Scaling data and parameters for a family of multi-modal large language models. *arXiv preprint arXiv:2402.05935*, 2024. 1, 3

[65] Fangyu Liu, Guy Emerson, and Nigel Collier. Visual spatial reasoning. *Transactions of the Association for Computational Linguistics*, 11:635–651, 2023. 5

[66] Fuxiao Liu, Xiaoyang Wang, Wenlin Yao, Jianshu Chen, Kaiqiang Song, Sangwoo Cho, Yaser Yacoob, and Dong Yu. Mmc: Advancing multimodal chart understanding with large-scale instruction tuning. *arXiv preprint arXiv:2311.10774*, 2023. 5

[67] Haotian Liu, Chunyuan Li, Yuheng Li, and Yong Jae Lee. Improved baselines with visual instruction tuning. In *Proceedings of the IEEE/CVF Conference on Computer Vision and Pattern Recognition*, pages 26296–26306, 2024. 1, 2, 3, 7

[68] Haotian Liu, Chunyuan Li, Yuheng Li, Bo Li, Yuanhan Zhang, Sheng Shen, and Yong Jae Lee. Llava-next: Improved reasoning, ocr, and world knowledge. <https://llava-vl.github.io/blog/2024-05-10-llava-next-stronger-llms/>

//llava-v1.github.io/blog/2024-01-30-llava-next/, 2024. 1

[69] Haotian Liu, Chunyuan Li, Qingyang Wu, and Yong Jae Lee. Visual instruction tuning. *Advances in neural information processing systems*, 36, 2024. 1, 2, 3, 6, 7, 5

[70] Yuliang Liu, Zhang Li, Biao Yang, Chunyuan Li, Xucheng Yin, Cheng-lin Liu, Lianwen Jin, and Xiang Bai. On the hidden mystery of ocr in large multimodal models. *arXiv preprint arXiv:2305.07895*, 2023. 6

[71] Yuliang Liu, Zhang Li, Biao Yang, Chunyuan Li, Xucheng Yin, Cheng-lin Liu, Lianwen Jin, and Xiang Bai. On the hidden mystery of ocr in large multimodal models. *arXiv preprint arXiv:2305.07895*, 2023. 5

[72] Yuan Liu, Haodong Duan, Yuanhan Zhang, Bo Li, Songyang Zhang, Wangbo Zhao, Yike Yuan, Jiaqi Wang, Conghui He, Ziwei Liu, et al. Mmbench: Is your multimodal model an all-around player? In *European Conference on Computer Vision*, pages 216–233. Springer, 2025. 6

[73] Shangbang Long, Siyang Qin, Dmitry Panteleev, Alessandro Bissacco, Yasuhisa Fujii, and Michalis Raptis. Icdar 2023 competition on hierarchical text detection and recognition. *arXiv preprint arXiv:2305.09750*, 2023. 5

[74] Pan Lu, Liang Qiu, Jiaqi Chen, Tony Xia, Yizhou Zhao, Wei Zhang, Zhou Yu, Xiaodan Liang, and Song-Chun Zhu. Iconqa: A new benchmark for abstract diagram understanding and visual language reasoning. *arXiv preprint arXiv:2110.13214*, 2021. 5

[75] Pan Lu, Swaroop Mishra, Tony Xia, Liang Qiu, Kai-Wei Chang, Song-Chun Zhu, Oyvind Tafjord, Peter Clark, and Ashwin Kalyan. Learn to explain: Multimodal reasoning via thought chains for science question answering. In *The 36th Conference on Neural Information Processing Systems (NeurIPS)*, 2022. 5

[76] Pan Lu, Hritik Bansal, Tony Xia, Jiacheng Liu, Chunyuan Li, Hannaneh Hajishirzi, Hao Cheng, Kai-Wei Chang, Michel Galley, and Jianfeng Gao. Mathvista: Evaluating mathematical reasoning of foundation models in visual contexts. *arXiv preprint arXiv:2310.02255*, 2023. 6

[77] Shiyin Lu, Yang Li, Qing-Guo Chen, Zhao Xu, Weihua Luo, Kaifu Zhang, and Han-Jia Ye. Ovis: Structural embedding alignment for multimodal large language model. *arXiv:2405.20797*, 2024. 7

[78] Kenneth Marino, Mohammad Rastegari, Ali Farhadi, and Roozbeh Mottaghi. Ok-vqa: A visual question answering benchmark requiring external knowledge. In *Proceedings of the IEEE/cvf conference on computer vision and pattern recognition*, pages 3195–3204, 2019. 5

[79] Ahmed Masry, Do Xuan Long, Jia Qing Tan, Shafiq Joty, and Enamul Hoque. Chartqa: A benchmark for question answering about charts with visual and logical reasoning. *arXiv preprint arXiv:2203.10244*, 2022. 5

[80] Minesh Mathew, Lluis Gomez, Dimosthenis Karatzas, and CV Jawahar. Asking questions on handwritten document collections. *International Journal on Document Analysis and Recognition (IJDAR)*, 24(3):235–249, 2021. 5

[81] Minesh Mathew, Dimosthenis Karatzas, and CV Jawahar. Docvqa: A dataset for vqa on document images. In *Proceedings of the IEEE/CVF winter conference on applications of computer vision*, pages 2200–2209, 2021. 5

[82] Minesh Mathew, Viraj Bagal, Rubén Tito, Dimosthenis Karatzas, Ernest Valveny, and CV Jawahar. Infographicvqa. In *Proceedings of the IEEE/CVF Winter Conference on Applications of Computer Vision*, pages 1697–1706, 2022. 5

[83] Brandon McKinzie, Zhe Gan, Jean-Philippe Fauconnier, Sam Dodge, Bowen Zhang, Philipp Dufter, Dhruti Shah, Xianzhi Du, Futang Peng, Floris Weers, et al. Mm1: Methods, analysis & insights from multimodal llm pre-training. *arXiv preprint arXiv:2403.09611*, 2024. 3

[84] Kevin Meng, Arnab Sen Sharma, Alex Andonian, Yonatan Belinkov, and David Bau. Mass-editing memory in a transformer. *arXiv preprint arXiv:2210.07229*, 2022. 5

[85] Nitesh Methani, Pritha Ganguly, Mitesh M Khapra, and Pratyush Kumar. Plotqa: Reasoning over scientific plots. In *Proceedings of the IEEE/CVF Winter Conference on Applications of Computer Vision*, pages 1527–1536, 2020. 5

[86] Anand Mishra, Shashank Shekhar, Ajeet Kumar Singh, and Anirban Chakraborty. Ocr-vqa: Visual question answering by reading text in images. In *ICDAR*, 2019. 5

[87] Alec Radford, Jong Wook Kim, Chris Hallacy, Aditya Ramesh, Gabriel Goh, Sandhini Agarwal, Girish Sastry, Amanda Askell, Pamela Mishkin, Jack Clark, et al. Learning transferable visual models from natural language supervision. In *International conference on machine learning*, pages 8748–8763. PMLR, 2021. 1, 7

[88] Pranav Rajpurkar, Robin Jia, and Percy Liang. Know what you don’t know: Unanswerable questions for SQuAD. In *Proceedings of the 56th Annual Meeting of the Association for Computational Linguistics (Volume 2: Short Papers)*, pages 784–789, Melbourne, Australia, 2018. Association for Computational Linguistics. 5

[89] Machel Reid, Nikolay Savinov, Denis Teplyashin, Dmitry Lepikhin, Timothy Lillicrap, Jean-baptiste Alayrac, Radu Soricu, Angeliki Lazaridou, Orhan Firat, Julian Schrittwieser, et al. Gemini 1.5: Unlocking multimodal understanding across millions of tokens of context. *arXiv preprint arXiv:2403.05530*, 2024. 1, 3

[90] Olga Russakovsky, Jia Deng, Hao Su, Jonathan Krause, Sanjeev Satheesh, Sean Ma, Ziheng Huang, Andrej Karpathy, Aditya Khosla, Michael Bernstein, Alexander C. Berg, and Li Fei-Fei. ImageNet Large Scale Visual Recognition Challenge. *International Journal of Computer Vision (IJCV)*, 115(3):211–252, 2015. 5

[91] Sanket Shah, Anand Mishra, Naganand Yadati, and Partha Pratim Talukdar. Kvqa: Knowledge-aware visual question answering. In *Proceedings of the AAAI conference on artificial intelligence*, pages 8876–8884, 2019. 5

[92] Yuzhang Shang, Mu Cai, Bingxin Xu, Yong Jae Lee, and Yan Yan. Llava-prumerge: Adaptive token reduction for efficient large multimodal models. *arXiv preprint arXiv:2403.15388*, 2024. 3

[93] Hao Shao, Shengju Qian, Han Xiao, Guanglu Song, Zhuofan Zong, Letian Wang, Yu Liu, and Hongsheng Li. Visual

5
 cot: Unleashing chain-of-thought reasoning in multi-modal language models. *arXiv preprint arXiv:2403.16999*, 2024.

[94] Wenhao Shi, Zhiqiang Hu, Yi Bin, Junhua Liu, Yang Yang, See-Kiong Ng, Lidong Bing, and Roy Ka-Wei Lee. Math-llava: Bootstrapping mathematical reasoning for multimodal large language models. *arXiv preprint arXiv:2406.17294*, 2024. 5

[95] Oleksii Sidorov, Ronghang Hu, Marcus Rohrbach, and Amanpreet Singh. Textcaps: a dataset for image captioning with reading comprehension. 2020. 5

[96] Amanpreet Singh, Vivek Natarajan, Meet Shah, Yu Jiang, Xinlei Chen, Dhruv Batra, Devi Parikh, and Marcus Rohrbach. Towards vqa models that can read. In *Proceedings of the IEEE/CVF conference on computer vision and pattern recognition*, pages 8317–8326, 2019. 6, 5

[97] Dominik Stammbach and Elliott Ash. Docscan: Unsupervised text classification via learning from neighbors. *arXiv preprint arXiv:2105.04024*, 2021. 5

[98] Hamed Rahimi Sujet AI, Allaa Boutaleb. Sujet-finance-qavision-100k: A large-scale dataset for financial document vqa, 2024. 5

[99] S Svetlichnaya. Deepform: Understand structured documents at scale. 2020. 5

[100] Ryota Tanaka, Kyosuke Nishida, and Sen Yoshida. Visualmrc: Machine reading comprehension on document images. In *Proceedings of the AAAI Conference on Artificial Intelligence*, pages 13878–13888, 2021. 5

[101] Shengbang Tong, Ellis Brown, Penghao Wu, Sanghyun Woo, Manoj Middepogu, Sai Charitha Akula, Jihan Yang, Shusheng Yang, Adithya Iyer, Xichen Pan, et al. Cambrian-1: A fully open, vision-centric exploration of multimodal llms. *arXiv preprint arXiv:2406.16860*, 2024. 3, 7

[102] Hugo Touvron, Thibaut Lavril, Gautier Izacard, Xavier Martinet, Marie-Anne Lachaux, Timothée Lacroix, Baptiste Rozière, Naman Goyal, Eric Hambro, Faisal Azhar, et al. Llama: Open and efficient foundation language models. *arXiv preprint arXiv:2302.13971*, 2023. 1

[103] Andreas Veit, Tomas Matera, Lukas Neumann, Jiri Matas, and Serge Belongie. Coco-text: Dataset and benchmark for text detection and recognition in natural images. *arXiv preprint arXiv:1601.07140*, 2016. 5

[104] Aladin Virmaux and Kevin Scaman. Lipschitz regularity of deep neural networks: analysis and efficient estimation. *Advances in Neural Information Processing Systems*, 31, 2018. 2

[105] Peng Wang, Shuai Bai, Sinan Tan, Shijie Wang, Zhihao Fan, Jinze Bai, Keqin Chen, Xuejing Liu, Jialin Wang, Wenbin Ge, et al. Qwen2-vl: Enhancing vision-language model’s perception of the world at any resolution. *arXiv preprint arXiv:2409.12191*, 2024. 1

[106] Weihang Wang, Qingsong Lv, Wenmeng Yu, Wenyi Hong, Ji Qi, Yan Wang, Junhui Ji, Zhuoyi Yang, Lei Zhao, Xixuan Song, Jiazheng Xu, Bin Xu, Juanzi Li, Yuxiao Dong, Ming Ding, and Jie Tang. Cogvilm: Visual expert for pretrained language models, 2023. 5

[107] Yi Wang, Yinan He, Yizhuo Li, Kunchang Li, Jiashuo Yu, Xin Ma, Xinhao Li, Guo Chen, Xinyuan Chen, Yaohui Wang, Conghui He, Ping Luo, Ziwei Liu, Yali Wang, Limin Wang, and Yu Qiao. Internvid: A large-scale video-text dataset for multimodal understanding and generation, 2024. 5

[108] Haoran Wei, Lingyu Kong, Jinyue Chen, Liang Zhao, Zheng Ge, Jinrong Yang, Jian-Yuan Sun, Chunrui Han, and Xiangyu Zhang. Vary: Scaling up the vision vocabulary for large vision-language models. *ArXiv*, abs/2312.06109, 2023. 3

[109] Yuxin Wen, Qingqing Cao, Qichen Fu, Sachin Mehta, and Mahyar Najibi. Efficient vision-language models by summarizing visual tokens into compact registers. *arXiv preprint arXiv:2410.14072*, 2024. 1, 2

[110] C. Wendler. Renderedtext. <https://huggingface.co/datasets/wendlerc/RenderedText>, 2023. 5

[111] Jianshu Chen Yunkai Zhang Hong Wang Shiyang Li Xiyou Zhou Wenhua Chen, Hongmin Wang and William Yang Wang. Tabfact : A large-scale dataset for table-based fact verification. In *International Conference on Learning Representations (ICLR)*, Addis Ababa, Ethiopia, 2020. 5

[112] Ruyi Xu, Yuan Yao, Zonghao Guo, Junbo Cui, Zanlin Ni, Chunjiang Ge, Tat-Seng Chua, Zhiyuan Liu, Maosong Sun, and Gao Huang. Llava-uhd: an lmm perceiving any aspect ratio and high-resolution images. *arXiv preprint arXiv:2403.11703*, 2024. 1, 3

[113] Zhengzhuo Xu, Sinan Du, Yiyuan Qi, Chengjin Xu, Chun Yuan, and Jian Guo. Chartbench: A benchmark for complex visual reasoning in charts. *arXiv preprint arXiv:2312.15915*, 2023. 5

[114] An Yang, Baosong Yang, Binyuan Hui, Bo Zheng, Bowen Yu, Chang Zhou, Chengpeng Li, Chengyuan Li, Dayiheng Liu, Fei Huang, et al. Qwen2 technical report. *arXiv preprint arXiv:2407.10671*, 2024. 3

[115] Senqiao Yang, Yukang Chen, Zhuotao Tian, Chengyao Wang, Jingyao Li, Bei Yu, and Jiaya Jia. Visionzip: Longer is better but not necessary in vision language models. *arXiv preprint arXiv:2412.04467*, 2024. 4

[116] Linli Yao, Lei Li, Shuhuai Ren, Lean Wang, Yuanxin Liu, Xu Sun, and Lu Hou. Deco: Decoupling token compression from semantic abstraction in multimodal large language models. *arXiv preprint arXiv:2405.20985*, 2024. 1

[117] Yuan Yao, Tianyu Yu, Ao Zhang, Chongyi Wang, Junbo Cui, Hongji Zhu, Tianchi Cai, Haoyu Li, Weilin Zhao, Zhihui He, et al. Minicpm-v: A gpt-4v level mllm on your phone. *arXiv preprint arXiv:2408.01800*, 2024. 3, 7

[118] Jiabo Ye, Haiyang Xu, Haowei Liu, Anwen Hu, Ming Yan, Qi Qian, Ji Zhang, Fei Huang, and Jingren Zhou. mplug-owl3: Towards long image-sequence understanding in multi-modal large language models. *arXiv preprint arXiv:2408.04840*, 2024. 7

[119] Xubing Ye, Yukang Gan, Xiaoke Huang, Yixiao Ge, Ying Shan, and Yansong Tang. Voco-llama: Towards vision compression with large language models. *arXiv preprint arXiv:2406.12275*, 2024. 1

[120] Tianyu Yu, Haoye Zhang, Yuan Yao, Yunkai Dang, Da Chen, Xiaoman Lu, Ganqu Cui, Taiwen He, Zhiyuan Liu,

Tat-Seng Chua, and Maosong Sun. Rlaif-v: Aligning mllms through open-source ai feedback for super gpt-4v trustworthiness. *arXiv preprint arXiv:2405.17220*, 2024. 5

[121] Weihao Yu, Zhengyuan Yang, Linjie Li, Jianfeng Wang, Kevin Lin, Zicheng Liu, Xinchao Wang, and Lijuan Wang. Mm-vet: Evaluating large multimodal models for integrated capabilities. *arXiv preprint arXiv:2308.02490*, 2023. 6

[122] Xinyan Velocity Yu, Sewon Min, Luke Zettlemoyer, and Hannaneh Hajishirzi. Crepe: Open-domain question answering with false presuppositions. *arXiv preprint arXiv:2211.17257*, 2022. 5

[123] Zhengqing Yuan, Zhaoxu Li, Weiran Huang, Yanfang Ye, and Lichao Sun. Tinygpt-v: Efficient multimodal large language model via small backbones. *arXiv preprint arXiv:2312.16862*, 2023. 3

[124] Xiang Yue, Yuansheng Ni, Kai Zhang, Tianyu Zheng, Ruqi Liu, Ge Zhang, Samuel Stevens, Dongfu Jiang, Weiming Ren, Yuxuan Sun, et al. Mmmu: A massive multi-discipline multimodal understanding and reasoning benchmark for expert agi. In *Proceedings of the IEEE/CVF Conference on Computer Vision and Pattern Recognition*, pages 9556–9567, 2024. 6

[125] Chi Zhang, Feng Gao, Baoxiong Jia, Yixin Zhu, and Song-Chun Zhu. Raven: A dataset for relational and analogical visual reasoning. In *Proceedings of the IEEE/CVF conference on computer vision and pattern recognition*, pages 5317–5327, 2019. 5

[126] Renrui Zhang, Dongzhi Jiang, Yichi Zhang, Haokun Lin, Ziyu Guo, Pengshuo Qiu, Aojun Zhou, Pan Lu, Kai-Wei Chang, Peng Gao, et al. Mathverse: Does your multi-modal llm truly see the diagrams in visual math problems? *arXiv preprint arXiv:2403.14624*, 2024. 5

[127] Ying Zhang, Lionel Gueguen, Ilya Zharkov, Peter Zhang, Keith Seifert, and Ben Kadlec. Uber-text: A large-scale dataset for optical character recognition from street-level imagery. In *SUNw: Scene Understanding Workshop- CVPR*, page 5, 2017. 5

[128] Zhenyu Zhang, Ying Sheng, Tianyi Zhou, Tianlong Chen, Lianmin Zheng, Ruisi Cai, Zhao Song, Yuandong Tian, Christopher Ré, Clark Barrett, et al. H2o: Heavy-hitter oracle for efficient generative inference of large language models. *Advances in Neural Information Processing Systems*, 36:34661–34710, 2023. 3

[129] Bo Zhao, Boya Wu, Muyang He, and Tiejun Huang. Svit: Scaling up visual instruction tuning. *arXiv preprint arXiv:2307.04087*, 2023. 5

[130] Baichuan Zhou, Ying Hu, Xi Weng, Junlong Jia, Jie Luo, Xien Liu, Ji Wu, and Lei Huang. Tinyllava: A framework of small-scale large multimodal models. *arXiv preprint arXiv:2402.14289*, 2024. 3

[131] Deyao Zhu, Jun Chen, Xiaoqian Shen, Xiang Li, and Mohamed Elhoseiny. Minigpt-4: Enhancing vision-language understanding with advanced large language models. *arXiv preprint arXiv:2304.10592*, 2023. 3

[132] Fengbin Zhu, Wenqiang Lei, Youcheng Huang, Chao Wang, Shuo Zhang, Jiancheng Lv, Fuli Feng, and Tat-Seng Chua. Tat-qa: A question answering benchmark on a hybrid of tabular and textual content in finance. *arXiv preprint arXiv:2105.07624*, 2021. 5

[133] Yichen Zhu, Minjie Zhu, Ning Liu, Zhicai Ou, Xiaofeng Mou, and Jian Tang. Llava-\phi: Efficient multi-modal assistant with small language model. *arXiv preprint arXiv:2401.02330*, 2024. 3

Skip-Vision: Efficient and Scalable Acceleration of Vision-Language Models via Adaptive Token Skipping

Supplementary Material

8. Proof and detailed analysis of Skip-Vision

In this section, we provide a theoretical analysis to justify the rationale behind Skip-Vision and quantify the performance loss introduced by skipping FFN computations for redundant visual tokens.

8.1. Bounded error of Skip FFN

At the core of this analysis lies the layer error incurred when bypassing the FFN layer. For a given layer l , the original output $h_{\text{original}}^{(l)}$ is :

$$h_{\text{original}}^{(l)} = h_{\text{attn}}^{(l)} + \text{FFN}^{(l)}(h_{\text{attn}}^{(l)}). \quad (14)$$

When skipping the FFN, the output becomes:

$$h_{\text{skip}}^{(l)} = h_{\text{attn}}^{(l)}. \quad (15)$$

The per-layer skipping error is:

$$\epsilon^{(l)} = \|h_{\text{original}}^{(l)} - h_{\text{skip}}^{(l)}\|_2 = \|\text{FFN}^{(l)}(h_{\text{attn}}^{(l)})\|_2. \quad (16)$$

For redundant tokens, such as those in homogeneous image regions, this error is negligible ($\epsilon^{(l)} \approx 0$) due to minimal feature transformations by the FFN.

However, errors propagate through subsequent layers, amplified by the recursive nature of transformer architectures. Leveraging Lipschitz continuity assumptions for self-attention and FFN operations ($L_{\text{attn}}^{(l+1)}$ and $L_{\text{FFN}}^{(l+1)}$), the cumulative error at layer $l+1$ is bounded by:

$$\epsilon^{(l+1)} \leq (L_{\text{attn}}^{(l+1)} + L_{\text{FFN}}^{(l+1)}) \cdot \epsilon^{(l)} + \epsilon_{\text{skip}}^{(l+1)}, \quad (17)$$

where ($\epsilon_{\text{skip}}^{(l+1)}$ represents new errors from skipping deeper layers $(l+1)$).

Over L layers, the total error telescopes to:

$$\epsilon_{\text{total}} \leq \sum_{l=1}^L \epsilon_{\text{skip}}^{(l)} \cdot \prod_{i=1}^{L-l} (L_{\text{attn}}^{(i+1)} + L_{\text{FFN}}^{(i+1)}). \quad (18)$$

Theorem 8.1 Lipschitz Constants for Causal Attention and FFN in Transformers Assume:

1. Inputs are normalized (e.g., via LayerNorm), bounding intermediate feature norms.
2. Weight matrices in attention (W_Q, W_K, W_V) and FFN (W_1, W_2) have bounded spectral norms (maximum singular values).

Then the Lipschitz constants of these components satisfy:

1. Causal Attention:

$$L(\text{Attn}) \leq \frac{\|W_Q\|_2 \|W_K\|_2 \|W_V\|_2}{\sqrt{d_k}}, \quad (19)$$

where d_k is the key dimension. The causal mask further restricts attention dependencies, preserving this bound.

2. Feed - Forward Network (FFN):

$$L(\text{FFN}) \leq \|W_1\|_2 \|W_2\|_2, \quad (20)$$

assuming the activation function (e.g., ReLU, GELU) is 1-Lipschitz.

Proof.

The Lipschitz constant of causal attention

1. Linear Transformation:

The input sequence $X \in \mathbb{R}^{n \times d}$ undergoes three linear transformations to obtain the query $Q = XW_Q$, the key $K = XW_K$, and the value $V = XW_V$. The Lipschitz constant of each linear transformation is the spectral norm (the largest singular value) of its weight matrix, denoted as $\sigma_Q = \|W_Q\|_2$, $\sigma_K = \|W_K\|_2$, and $\sigma_V = \|W_V\|_2$ respectively.

2. Attention Score Calculation:

The scaled dot - product $S = QK^\top / \sqrt{d_k}$. The Lipschitz constant of the bilinear mapping is related to σ_Q and σ_K . If the norm of the input X is bounded (for example, through LayerNorm), then:

$$\text{Lip}(S) \leq \frac{\sigma_Q \sigma_K}{\sqrt{d_k}}. \quad (21)$$

3. Softmax Activation:

After applying the causal mask, softmax is performed on each row. The Lipschitz constant of Softmax under the ℓ_2 norm is less than 1, that is:

$$\text{Lip}(\text{softmax}) \leq 1. \quad (22)$$

4. Weighted Sum of Values: The output $\text{Attn}(X) = AV$, where $A = \text{softmax}(S)$. The Lipschitz constant of this step is determined by the spectral norm σ_V of the linear transformation of V .

Overall Lipschitz Constant

Combining the upper bounds of each step:

$$\text{Lip}(\text{CausalAttention}) \leq \frac{\sigma_Q \sigma_K \sigma_V}{\sqrt{d_k}}. \quad (23)$$

Impact of Causal Mask: The mask restricts the attention range, which may reduce the sensitivity to the input.

Therefore, the actual Lipschitz constant will not exceed the above-mentioned upper bound.

The Lipschitz Constant of FFN

The FFN is usually expressed as:

$$\text{FFN}(x) = W_2 \cdot \text{Activation}(W_1 x + b_1) + b_2, \quad (24)$$

where the Lipschitz constant of activation functions (such as ReLU, GELU) is 1.

Derivation of Lipschitz Constant

1. Linear Layer W_1 : The spectral norm is $\sigma_1 = \|W_1\|_2$.
2. Activation Function: $\text{Lip}(\text{Activation}) = 1$.
3. Linear Layer W_2 : The spectral norm is $\sigma_2 = \|W_2\|_2$.

Follow the equation 7 in [104], the overall Lipschitz constant is the product of the spectral norms of the two linear layers:

$$\text{Lip}(\text{FFN}) \leq \sigma_1 \sigma_2. \quad (25)$$

□

Corollary 8.1 Bounded Lipschitz If W_Q, W_K, W_V, W_1, W_2 are orthogonal matrices (spectral norm = 1), then:

- $L(\text{attn}) \leq 1/\sqrt{d_k}$
- $L(\text{FFN}) \leq 1$

If we assume Lipschitz constants $L_{\text{attn}} + L_{\text{FFN}} \leq \gamma$ and skipping errors $\epsilon_{\text{skip}}^{(l)} \leq \epsilon$, the total error is scaled to:

$$\epsilon_{\text{total}} \leq \epsilon \cdot \frac{\gamma^L - 1}{\gamma - 1}, \quad (26)$$

Theorem 5.1 establish that the skip error is bounded when $\gamma < 1$, provided the model is trained with modern regularization techniques. This ensures that the Multimodal Large Language Model (MLLM) remains less sensitive to the effects of skipping.

This error also impacts the KL divergence between the original and skipped outputs, bounded by:

$$\mathcal{D}_{\text{KL}}(p_{\text{skip}} \parallel p_{\text{original}}) \leq \frac{1}{2\sigma^2} \cdot \epsilon_{\text{total}}^2, \quad (27)$$

where σ^2 is the variance of the logits.

Proof. For two Gaussian distributions $p = \mathcal{N}(\mu_p, \Sigma_p)$ and $q = \mathcal{N}(\mu_q, \Sigma_q)$, their KL divergence is:

$$\begin{aligned} \mathcal{D}_{\text{KL}}(p \parallel q) &= \frac{1}{2}(\text{tr}(\Sigma_q^{-1} \Sigma_p) + (\mu_q - \mu_p)^T \Sigma_q^{-1} (\mu_q - \mu_p) \\ &\quad - k + \ln \frac{|\Sigma_q|}{|\Sigma_p|}) \end{aligned} \quad (28)$$

where k is the dimension. If we assume that the covariances of the two distributions are the same, i.e., $\Sigma_p = \Sigma_q = \sigma^2 I$, and the total difference in means is ϵ_{total} , then:

$$\mathcal{D}_{\text{KL}}(p \parallel q) = \frac{1}{2\sigma^2} \|\mu_p - \mu_q\|^2. \quad (29)$$

Here, $\|\mu_p - \mu_q\|^2$ is $\epsilon_{\text{total}}^2$, so:

$$\mathcal{D}_{\text{KL}}(p \parallel q) \leq \frac{1}{2\sigma^2} \epsilon_{\text{total}}^2. \quad (30)$$

□

Further integrating feature similarity errors ($\epsilon_{\text{sim}} = O(\sqrt{1-\theta})$) from low-attention tokens, the final bound becomes:

$$\mathcal{D}_{\text{KL}} \leq \frac{1}{2\sigma^2} \cdot (\epsilon_{\text{total}} + \epsilon_{\text{sim}})^2. \quad (31)$$

Practically, this analysis motivates a layer-wise skipping strategy, alongside token selection and token merge based on feature similarity (θ).

9. More experimental results

9.1. Efficiency.

Under the cos setting, we conduct more experiments to evaluate the training and inference efficiency. We compare with methods: FastV [21], Victor [109] and mean average pool, fine-tuning on LLaVA-665k using 8 NVIDIA A100 GPUs. As shown in Figure 11, our architecture outperforms in both metrics. Compared to the CoS_{1296} baseline, it achieves comparable performance with 35% less training time and 74% reduced inference computation. FastV, unable to utilize flash attention, shows a significant disadvantage, even surpassing baseline training time.

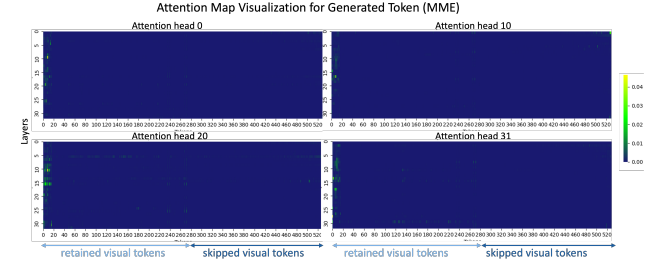


Figure 9. Visualization of attention map in MME.

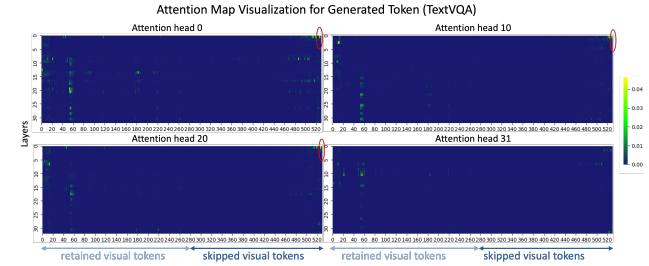


Figure 10. Visualization of attention map in TextVQA.

9.2. Ablation study

To validate the effectiveness of each component within the Skip-Vision framework, under CoS setting, we conducted

	SF	FS	LS	Merge	LV	SK	MME	Textvqa	MMB	MMVet	MMMU	MathV	OCRB	MMStar	Overall
0	<i>CoS₁₂₉₆</i>						1585	64.4	77.1	39.4	39.2	21.5	39.2	41.2	46
1				✓			1548	64.5	75.3	39.7	39.1	21.8	37.7	40.9	45.6
2	✓						1589	63.6	74.4	36.9	38	19.8	365	39.8	44.2
3	✓					✓	1591	63.7	74.9	39.4	38.7	20.7	36.3	39.9	44.8
4	✓			✓			1560	63.8	75.5	39.0	39.2	21	37.1	40.0	45.0
5	✓			✓		✓	1580	63.5	74.2	40.6	39.2	21.6	37.2	40.9	45.3
6	✓		✓	✓			1570	63.5	74.1	40	39.8	20.1	39	41.4	45.4
7	✓		✓	✓	✓		1593	62.6	74.7	40.3	40.2	21.6	36.6	41.1	45.3
8	✓		✓	✓	✓		1571	63.6	75.9	40.3	40.3	21	36.1	41.5	45.6
9	✓		✓	✓	✓	✓	1547	64.0	75.9	38	41.2	21.9	36.9	40.6	45.5
10	✓		✓	✓	✓	✓	1562	63.9	76.5	40.2	40.2	21.2	37.2	41.9	45.9
11	✓		✓	✓	✓	✓	1563	63.7	76.5	41.7	40.3	21.2	37.0	41.9	46

Table 5. **Ablation study.** To establish a strong baseline, we performed an ablation study on each component of the Skip-Vision framework with the LLaVA 665k SFT dataset. SF (skip FFN), FS (former summary token), LS (latter summary token), Merge (reducing local visual tokens from 1024 to 256), LV (passing the last local visual token through the FFN), SK (using skip KV-cache during inference). This analysis highlights the distinct contributions of each element to efficiency and performance.

Inference method	Skip window size	MME	Textvqa	MMB	MMVet	MMMU	MathV	OCRB	MMStar	Overall
Without skip KV-cache	-	1562	63.9	76.5	40.2	40.2	21.2	37.2	41.9	45.9
Skip KV-cache	middle+small	1562	61.8	76.5	32.6	40.4	21.2	22.6	41.9	42.4
Skip KV-cache	small	1563	63.7	76.5	41.7	40.3	21.2	37.0	41.9	46

Table 6. **Ablation study of skip KV-cache.** We report skip KV-cache performance across different visual token window sizes. Skip-Vision enables task-specific optimization by adjusting skip KV-cache levels for tailored acceleration.

ablation and comparative experiments on the skip FFN, summary token, token merge, last visual token, and skip KV-cache. The detailed experimental results are presented in the table 5.

The last summary token or final visual token must pass through the FFN. As discussed in Section 4.2, the final visual token plays a crucial role in predicting the subsequent text token, thereby requiring access to the textual knowledge encoded within the FFN layers. This integration of information is essential. Compare (2, 3, 4, 5) in Table 5, employing a summary token as the final visual token has demonstrated enhanced effectiveness compared to a standard visual token. Furthermore, our experimental findings reveal that optimal performance is achieved when both the summary token and the last local visual token are processed through the FFN.

The former summary token enhances the model’s comprehension of overall visual information. Compare (4,6), (7,8), (9,10) in Table 5, the former summary token enhances the emphasis on crucial information by adaptively merging large-scale visual features. This approach addresses the challenge posed by overly lengthy sequences of visual tokens bypassing the FFN, which may result in the omission of critical large-scale visual context.

The local token merge strategy seamlessly aligns with the skip-vision framework. Compare (0,1), (4,7), (6,8)

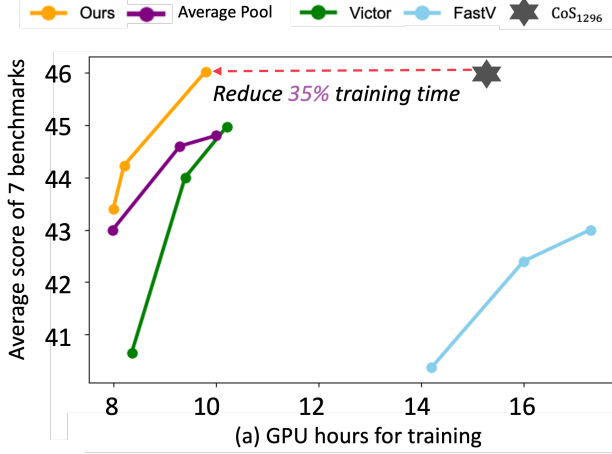
in Table 5, when local token merge is directly applied to the *CoS₁₂₉₆* baseline, the model’s overall performance declines, reflecting its dependency on redundant visual data when all tokens pass through the FFN. In contrast, within the skip-vision framework, merging local tokens results in improved performance, indicating that our architecture efficiently leverages visual information without requiring excessive redundancy.

The skip KV-cache mechanism enables adaptive selection of visual tokens to skip based on task-specific information requirements. As demonstrated in Table 6, for tasks such as MMB, MMU, and MMStar that do not necessitate fine-grained information, both middle and small window-size visual tokens can be skipped, with only the initial and final summary tokens retained. For detail-sensitive tasks like TextVQA and OCRBench, we skip only the small window-size tokens that bypass the FFN, thereby preserving critical fine-grained details. Applying skip KV-cache with small window-size tokens during inference improves performance, particularly in tasks requiring extended responses, such as MMVet.

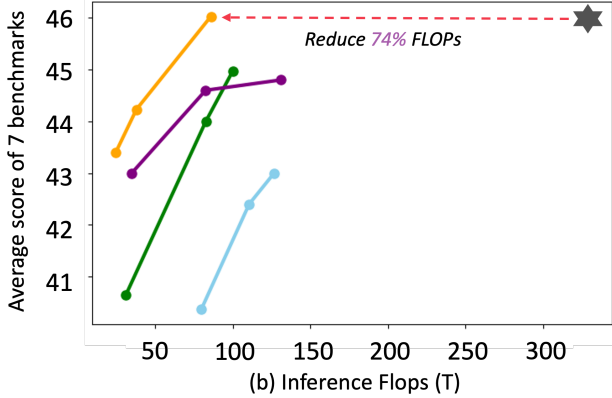
9.3. More visualizations

9.4. Dataset

In Table 7 and Table 8, we introduce the two scaling datasets used by Skip-Vision during the SFT stage: SK-1M and SK-



(a) GPU hours for training



(b) Inference Flops (T)

Figure 11. Performance vs. Training-Time and Inference FLOPs. Under the cos setting, we compare Skip-Vision with three MLLM acceleration methods, showing clear advantages in training speed and inference efficiency under equivalent computational constraints.

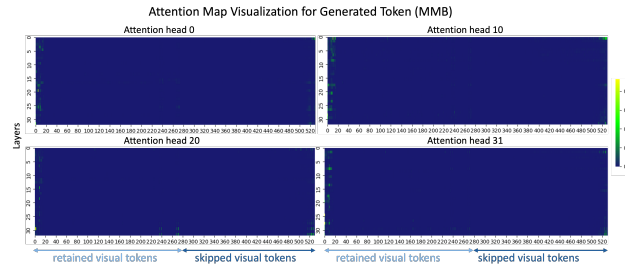


Figure 12. Visualization of attention map in MMBench.

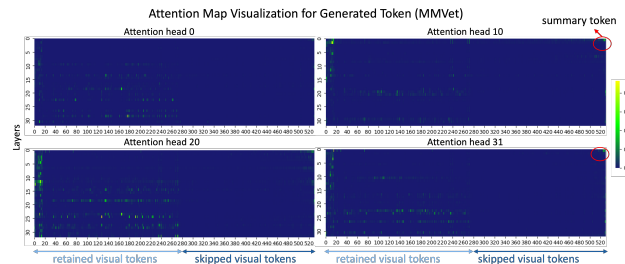


Figure 13. Visualization of attention map in MMVet.

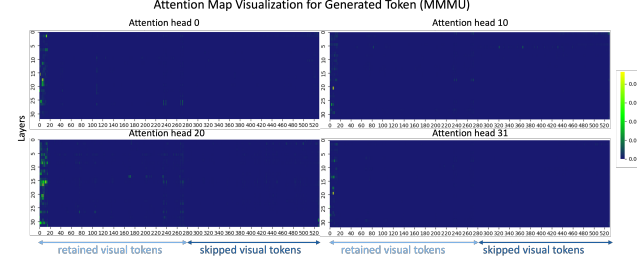


Figure 14. Visualization of attention map in MMMU.

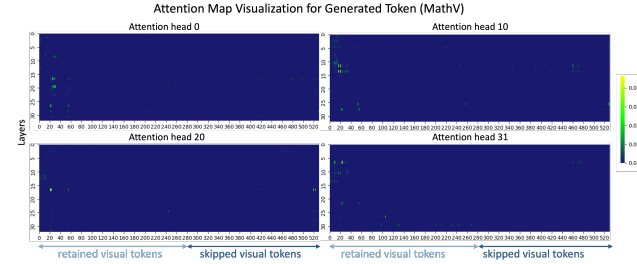


Figure 15. Visualization of attention map in MathV.

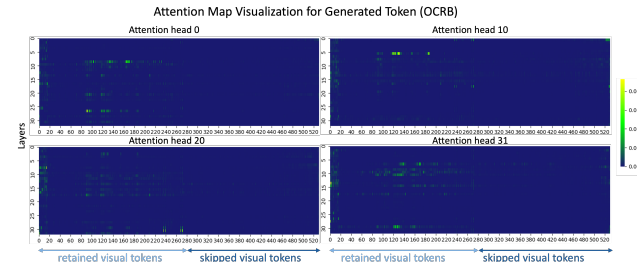


Figure 16. Visualization of attention map in OCRBench.

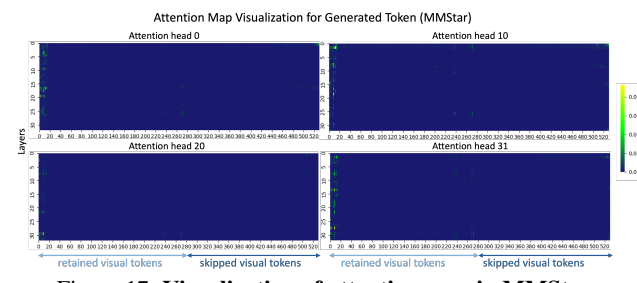


Figure 17. Visualization of attention map in MMStar.

Task	Dataset
Visual Instruction Tuning	LLaVA-665k [69], SVIT [129]
VQA	CREPE [122], Imagenet multi task [90], VQA-rad [52]
Visual Reasoning	Wikitable [51], Super-CLEVR [62], VSR [65]
Knowledge	ViQuAE [55], Kvqa [91], Websrc [22]
Chart / Diagram / graph	ChartQA [79], Iconqa [74], Infographicvqa [82],
Document	DeepForm [99], TAT-QA [132], Visualmrc [100], Docvqa [81], Sujet-Finance-QA-Vision-100k [98]
Math	Mathverse [126]
OCR / Screen / Scene text	TQA [50], HW-SQuAD [80], TextVQA [96], ST-VQA [8], TextOCR-GPT4V [13], OCRbench-kv [71], Uber-text [127]
Science	AI2D [49]

Table 7. Datasets used by SK-1M at the SFT stage.

Task	Dataset
Visual Instruction Tuning	SVIT [129], ALLaVA [17], ShareGPT4V [19], cog-vlm-sft [106]
Caption	TextCaps [95], ShareGPT-4o [107]
VQA	CREPE [122], Imagenet multi task [90], VQA-rad [52], VQAv2 [4], Vizwiz [33]
Visual Reasoning	Wikitable [51], Super-CLEVR [62], VSR [65], FigureQA [45], TallyQA [1], Visual cot [93], CLEVR [43], Raven [125]
Knowledge	ViQuAE [55], Kvqa [91], Websrc [22], OK-VQA [78], Volcano [54], RLAIF-V [120]
Chart / Diagram / graph	ChartQA [79], Iconqa [74], Infographicvqa [82], MapQA [16], TabFact [111], Chart2Text [46], DVQA [44], Chartbench [113], MMC [66]
Document	DeepForm [99], TAT-QA [132], Visualmrc [100], Docvqa [81], Sujet-Finance-QA-Vision-100k [98], Docmatix [53], DocReason25K [37], DocStruct4M [38]
Math	Mathverse [126], MathOCR [15], MathV360K [94], GeoGPT4V [11], Geo170K QA [30]
OCR / Screen / Scene text	TQA [50], HW-SQuAD [80], TextVQA [96], ST-VQA [8], TextOCR-GPT4V [13], OCRbench-kv [71], Uber-text [127], OCR-VQA [86], ScreenQA [5], SynthText [32], ChromeWriting [110], K12 Printing [57], SQuAD [88], ICDAR19-LSVT [48], ICPR18-MTWI [35], ICDAR19-ArT [25], COCO-Text [103], Docscan [97], HierText [73]
Science	AI2D [49], Plotqa [85], ArXivQA [59], ScienceQA [75]

Table 8. Datasets used by SK-9M at the SFT stage.